AUTOMATIC TOOTH DETECTION AND LABELLING FROM PANAROMIC RADIOGRAPHIC IMAGES

by

Selma GÜZEL

A thesis submitted to

the Graduate School of Sciences and Engineering

of

Fatih University

in partial fulfillment of the requirements for the degree of

Master of Science

in

Computer Engineering

April 2014
Istanbul, Turkey

APPROVAL PAGE

This is to certify that I have read this thesis written by Selma GÜZEL and that in my opinion it is fully adequate, in scope and quality, as a thesis for the degree of Master of Science in Computer Engineering.

_____
Asst. Prof. Dr. Kadir TUFAN
Thesis Supervisor

_____
Asst. Prof. Dr. A.Betül OKTAY
Co-Supervisor

I certify that this thesis satisfies all the requirements as a thesis for the degree of Master of Science in Computer Engineering.

_____
Asst. Prof. Dr. Kadir TUFAN
Head of Department

Examining Committee Members

Asst. Prof. Dr. Kadir TUFAN _____

Asst. Prof. Dr. A.Betül OKTAY _____

Asst. Prof. Dr. Aişe Zülal ŞEVKLİ _____

Asst. Prof. Dr. Saime AKDEMİR AKAR _____

Asst. Prof. Dr. Zeynep ORHAN _____

It is approved that this thesis has been written in compliance with the formatting rules laid down by the Graduate School of Sciences and Engineering.

_____
Assoc. Prof. Dr. Nurullah ARSLAN
Director

April 2014

AUTOMATIC TOOTH DETECTION AND LABELLING FROM PANAROMIC RADIOGRAPHIC IMAGES

Selma GÜZEL

M.S. Thesis – Computer Engineering
April 2014

Thesis Supervisor: Assistant Prof. Dr. Kadir TUFAN

Co-Supervisor: Assistant Prof. Dr. A. Betül OKTAY

ABSTRACT

Detection and labelling are two fundemantal steps in most of the object identification systems. This thesis encapsulates the implementations of these processes which will be integrated to the prospective human identification system. The aim of this human identification system is identifying dead bodies after catastrophes by comparing the postmortem and the antemortem dental panoramic radiographs of the humans. The main reason of utilizing the dental information as biometric in this system, instead of other alternatives, is the durable structure of the tooth. Besides, the tooth has salient features which makes it appropriate to be detected. In addition, the relationships between the teeth on a radiographic image are also valuable to detect and to label the teeth accurately.

The tooth identification framework developed for this thesis consists of the detection and the labeling modules. The detection module detects the teeth using the SVM and the Boosting classifiers with the Haar and the HOG feature descriptors. After obtaining the candidate tooth locations by the detection module, the tooth numbering is carried out using the specific graphical modelling method with dynamic programming and the statistical optimization techniques by the labeling module. The tooth identification framework, including the detection and the labelling steps, is tested and evaluated on twenty panoromic radiographic test images and the results are promising.

Keywords: human identification, dental biometrics, feature extraction, object detection, labelling

PANAROMİK RADYOGRAFİK RESİMLERDEN DİŞLERİN OTOMATİK TESPİT EDİLMESİ VE ETİKETLENMESİ

Selma GÜZEL

Yüksek Lisans Tezi – Bilgisayar Mühendisliği
Nisan 2014

Tez Danışmanı: Yrd. Doç. Dr. Kadir TUFAN

Eş Danışman: Yrd. Doç. Dr. A. Betül OKTAY

ÖZ

Saptama ve etiketleme, çoğu nesne tanıma sistemlerinde iki temel adımdır. Bu tez, gelecekte yapılacak bir şahıs tanıma sistemine entegre edilecek olan bu işlemlerin implamantasyonunu kapsamaktadır. Bu şahıs tanıma sisteminin amacı, felaketlerden sonra, ölüm sonrası ve öncesindeki panoromik diş radyograflarının karşılaştırılarak ölü bedenlerin tanınmasıdır. Bu sistemde, biometrik olarak, diğer alternatiflerin yerine, diş bilgisinin kullanılmasının asıl amacı, dişin dayanıklı yapısıdır. Bunun yanında, diş, saptanabilecek belirgin özelliklere sahiptir. Ayrıca, radyorafik bir resimdeki, dişler arasındaki ilişkiler, dişlerin doğru bir şekilde saptanması ve özellikle etiketlenmesi için önem arz etmektedir.

Bu tez için geliştirilen diş tanıma sistemi, tanıma ve etiketleme olmak üzere iki modülden oluşmaktadır. Tanıma modülü, Haar ve HOG özellik tanımlayıcıları ile SVM ve Boosting metotlarını kullanarak dişleri tanır. Tanıma modülüyle aday diş lokasyonlarının elde edilmesinin ardından, etiketleme modülü tarafından, özel bir grafik modelleme metodunun, dinamik programlama ve istatistiksel en iyileme teknikleri ile kullanılması sonucu, dişler numaralandırılır. Bu, bizim de birincil katkımız olan, tanıma ve etiketleme işlemlerinin birleştirilmesinin, 20 panoramik radyografik test resmi üzerinde yeterli başarı sağladığı gözlemlenmiştir. Tanıma ve etiketleme adımlarını içeren diş tanıma sistemi, 20 panoramik radyografik test resmi üzerinde test edildi ve değerlendirildi; sonuçlar ümit verici.

Anahtar Kelimeler: Şahıs tanıma, diş biyometrikleri, özellik çıkarma, nesne tanıma, etiketleme

To all good people

ACKNOWLEDGEMENT

First of all, I would to like to thank my supervisor Kadir TUFAN for his help and strong encouragement.

I express appreciation to my co-adviser A.Betül OKTAY for her valuable guidance, recommendations and comments.

Lastly, Thanks to my parents for their understanding and motivation.

This project is supported by TÜBİTAK project named “113E1144- Human Identification using Dental Radiographs as Biometrics.”

TABLE OF CONTENTS

ABSTRACT iii
ÖZ iv
DEDICATION v
ACKNOWLEDGMENT vi
TABLE OF CONTENTS vii
LIST OF TABLES ix
LIST OF FIGURES x
LIST OF SYMBOLS AND ABBREVIATIONS xii
CHAPTER 1 INTRODUCTION 1
CHAPTER 2 LITERATURE REVIEW 4
CHAPTER 3 THE TOOTH IDENTIFICATION FRAMEWORK 8
CHAPTER 4 THE TOOTH DETECTION MODULE 12
4.1 Feature Extraction 13
4.1.1 Haar Filters 13
4.1.2 HOG Filters 14
4.2 Classificaiton. 16
4.1.1 Support Vector Machines (SVM) 16
4.1.2 Boosting 18
CHAPTER 5 THE TOOTH LABELLING MODULE 21
5.1 The Labelling Approach 21
5.1.1 The Graphical Tooth Model 21
5.1.2 The Labelling 23
5.2 The Components of The Model 29
CHAPTER 6 EXPERIMENTAL RESULTS 32
6.1 The Evaluation of the Tooth Detection Module 33
6.1.1 The Pre-processing 33
6.1.2 The Feature Extraction 33

6.1.3 The Classification Module 34
6.1.4 The Visual Detection Results 34
6.1.5 The Numerical Detection Results 35
6.1.6 The Discussion 36
6.2 The Evaluation of the Tooth Labelling Module 37
6.2.1 The Pre-processing 37
6.2.2 The Labelling Results 38
6.2.3 The Evaluation 43
6.2.4 Benchmarking with a Well-Known Method 48
6.2.5 The Discussion 53
CHAPTER 7 CONCLUSIONS 55
REFERENCES 57

LIST OF TABLES

TABLE

6.1 The numerical results of the detection module while using the SVM 36
6.2 The numerical results of the detection module while using the Boosting..... 36
6.3 The minimum and the maximum tooth widths used in the tooth models 37
6.4 The numerical results of the semi-automatic labelling based on the bi-cost 44
6.5 The numerical results of the semi-automatic labelling based on the d-cost..... 44
6.6 The numerical results of the fully-automatic labelling based on the d-cost..... 45
6.7 The numerical results of the fully-automatic labelling based on the d-cost..... 46
6.8 The numerical results of the method of W & F..... 49
6.9 The benchmarking with our methods and the method of W & F..... 51

LIST OF FIGURES

FIGURE

3.1 The tooth sets of a jaw ..... …9
3.2 The framework consists of the tooth detection and labeling modules 11
4.1 The Tooth Detection Module 12
4.2 Haar filters 14
4.3 The components of the HOG filter 15
4.4 C-HOG filters 16
4.5 Support vectors determining the best hyperplane 17
4.6 Transformation from input data space to a higher dimensional feature space 18
4.7 The boosting process 20
5.1 The proposed graphical tooth model for the right upper jaw 22
5.2 The best candidate tooth label selection 24
5.3 The h-approch and the v-approach for best tooth model selection 25
5.4 The bi-cost computation 26
5.5 The d-cost computation 27
5.6 The Tooth Labelling Module 31
6.1 A panoramic radiograph from the dataset used in the system 32
6.2 The visual results of the detection module using the Boosting method 34
6.3 The visual results of the detection module using the SVM method 35
6.4 The determination of the intersection of the mouth gap and the nose position 38
6.5 The visual result of the candidate labelling process for the left lower jaw 39
6.6 The visual results of the semi-automatic labelling method based on the bi-cost .. 40
6.7 The visual results of the semi-automatic labelling method based on the d-cost ... 41
6.8 The visual results of the fully-automatic labelling method based on the bi-cost .. 42
6.9 The visual results of the fully-automatic labelling method based on the d-cost ... 43
6.10 The visual results of three problematic images while labelling 47
6.11 The visual result of the method of Wanat and Frejlichowski 49

6.12 The visual results of the method of W&F for two problematic images 52
6.13 The Prospective Optimizer Based Labelling Approach 54

LIST OF SYMBOLS AND ABBREVIATIONS

SYMBOL/ABBREVIATION

ADIS	Automated Dental Identification System
CBCT	Cone Bean Computed Tomography
C-HOG	Circular HOG
CT	Computed Tomography
DIFT	Differentatial Image-Foresting Transform
HOG	Histogram of Oriented Gradients
OPENCV	Open Source Computer Vision Library
RBF	Radial Basis Function
R-HOG	Rectengular HOG
SMO	Sequential Minimal Optimization
SVM	Support Vector Machines
WEKA	Waikato Environment for Knowledge Analysis

CHAPTER 1

INTRODUCTION

Object identification is a fundamental step in most of the computer vision systems which perform planning, analysis, diagnosis, etc. An object to be used in these systems should have salient and invariant characteristics.

This thesis introduces the tooth identification stage of a prospective human identification system. In this system, dead bodies are identified by comparing their antemortem and postmortem dental radiographs. The first reason of selecting the tooth as the biometric is its distinguishing characteristics which are recognized even in unqualified images. The prospective human identification system is especially designed for finding dead bodies after catastrophes in which most of the human organs become unrecognizable or even disappeared. The second reason of preferring tooth as the biometric comes to play in this point; it is durable and therefore it is not damaged as much as the other structures which are also used as biometrics like fingerprint, iris, etc (Suteerayongprasert et al., 2007; Marana et al., 2011).

There are three basic types of dental radiographs used in the dentistry which are bitewing, periapical, and panoramic radiographs. The proposed system in this study works on the panoramic X-ray images. Despite of the fact that, the tooth structures are corrupted and the teeth are occluded due to the image stitching technique of panoramic imaging, these radiographs are preferred because of involving the whole mouth.

In this study, the teeth are divided into the tooth sets taking both the tooth classes and the tooth positions into account. There exist three classeses, which are molar, premolar, and incisor. The cuspids belong to the same sets with the incisors according to their positions. Namely, the proposed system accepts a panoramic image as a

combination of the regions where each region includes one tooth set. The system handles each of them separately.

The tooth identification system consists of two modules; the detection and the labeling modules. The detection module, which is based on the supervised machine learning, has two components which are the feature extraction and the classification.

The classification component implements the Support Vector Machines (SVM) (Welling, 2005) and Boosting (Freund and Schapire, 1999) algorithms to classify a tooth into one of the tooth sets. The classifiers run with the features of the Haar (Viola and Jones, 2001) and the Histogram of Oriented Gradients (HOG) (Seemann, 2008) extracted by the feature extraction module. They provide the shape and textural characteristics of teeth which are more representative than the local intensity information.

The labelling module of the system completes the identification process. A candidate tooth is labelled based on both its location and the locations of the adjacent teeth on the same horizontal region according to the intersection point of the jaws gap and the center of the first incisors. The labelling is performed using dynamic programming with the specific graphical modelling method and the statistical optimization techniques.

The contributions of this study are; (i) Comparing the accuracy rates of the two texture descriptors, the Haar and the HOG filters, for feature extraction, (ii) Evaluating the performance of the two machine learning algorithms, the SVM and the Boosting methods for classification, (iii) Integration of the detection and the labeling processes under the same framework, (iv) A novel labelling approach which uses dynamic programming and statistical optimization to numerate the teeth based on a specific numbering system.

The organization of this thesis is as follows: Chapter 2 reviews the literature on the tooth identification systems. Chapter 3 introduces the framework of the proposed system. Chapter 4 introduces the detection module of the proposed system. It presents the feature extraction and the classification components of this module. In this chapter, the Haar and the HOG filters as feature descriptors and, the SVM and Boosting

algorithms as classification methods are included. Chapter 5 explains the labelling module whichinvolves dynamic programming and statistical optimization. Chapter 6 presents the experimental results of our study and Chapter 7 concludes the thesis.

CHAPTER 2

LITERATURE REVIEW

In the literature, various tooth identification systems are presented. The fundamental steps in these systems are image enhancement, segmentation, and isolation. More sophisticated systems involve classification and labeling steps additionally.

In order to isolate the teeth in a dental radiograph appropriately, it is required to enhance and segment the image accurately. The proposed systems in the literature take this consideration into account to detect the teeth appropriately.

The Automated Dental Identification System (ADIS) of Abdel-mottaleb et al. (Abdel-mottaleb et al., 2006), which worked on the bitewing images, first, segmented the teeth from the background with the iterative and the adaptive thresholding techniques. Then, they splitted the jaws and isolated the teeth using the integral intensity projection method followed by the piece-wise function. This study is accepted as the pioneer in terms of the tooth isolation approach. Zhou and Abdel-mottaleb (Zhou and Abdel-mottaleb, 2005) employed the active contours (snakes) to isolate the teeth in advance of using the integral intensity projection to determine the initial contours. The method works on the bitewing images which were selected from all types of the dental radiographs via the Bayes classifier. Before actualizing the isolation, the images were enhanced using the morphological top-hat and the bottom-hat operations to emphasize the tooth structure. Jain and Chen (Jain and Chen, 2004) also used the same method for tooth isolation. Then, they extracted the contour of the tooth crown by drawing lines from the center of it and applying the Bayesian rule to determine if the pixel on the line is a contour pixel or not. After that, starting from the right and the left ends of the crown contour, the contour of the root was extracted such that the pixel on the root contour

separates the particular neighborhood of the background pixel from the particular technique after the integral intensity projection method to isolate the teeth. The best window sizes of the teeth used in this technique were determined with the adaptive windowing algorithm. In this study, the missing teeth were detected using the first derivatives of the vertical projections. In addition, this system eliminated the inaccurate segmentation lines by considering the location of a distinctive region within a tooth, the dental pulp. This region was also utilized in the study of Wanat and Frejlichowski (Wanat and Frejlichowski, 2011a) instead of the gaps between the teeth for separating the adjacent teeth while employing the integral intensity projection automatically to isolate the teeth. Preparatory to this process, jaw splitting line was moved vertically up to the pulp detection occurs. In addition, a second point was found within the probable gap region between the teeth using the greedy technique taking the slope of the separation line into account. Furthermore, the ending line separating the tooth root from the checkbone was determined with the similar approach implemented to the pulp line. The inaccurate tooth separation lines were eliminated based on the average tooth size. Another study Fahmy et al. (Fahmy et al., 2004) using the integral intensity projection to isolate the teeth, extracts several features from the contours of the isolated teeth, such as the shape and the size of each tooth, and the tooth root characteristics, for further processes. The missing teeth were found using the space between the adjacent teeth. Marana et al. (Marana et al., 2011) applied the integral intensity projection with the snakes to the panoramic images for detecting the dental work. In addition, the Differentatial Image-Foresting Transform (DIFT) was tested for the same purpose alternatively. In their system, Pushparaj et al. (Pushparaj et al., 2013) applied the Butterworth high pass filter and the homomorphic filter to the dental radiographs for making the images sensitive to the all frequencies and illuminated uniformly before isolating the teeth using the integral intensity projection. After the isolation, the labelling of the teeth was performed using the connected component and the fast connected component methods.

In the literature, the method of the integral intensity projection is also used in more complex systems, which involve the classification and the numbering processes, to isolate the teeth. One example of such systems is the study of the Yuniarti et al. (Yuniarti et al, 2012). In this study, after enhancing the panoramic or bitewing images with the top-hat and the bottom-hat operators and the local histogram equalization, the

teeth were isolated and then the SVM classifier run with the features such as the tooth area, the ratio of height to width and the tooth centroid, to classify a tooth as a molar or a pre-molar. The tooth identification was completed after labelling the teeth according to a particular pattern. Lin et al. (Lin et al., 2010) also used the SVM algorithm in their proposed system to classify molars and pre-molars. The SVM classifier of this system used the relative length/width, the relative pulp length/width and the relative crown size as features which were extracted from the bitewing images with the iterative thresholding and the B-spline techniques. The images were enhanced by the homorphic filtering, the adaptive contrast stretching and the adaptive morphological transformations in the pre-processing stage of the system. However, this system did not have a labelling component. Jain and Chen (Jain and Chain, 2005) presented a system in which the SVM algorithm was used for classifying a tooth as a molar, a (bi) cuspid or an incisor. In this study, they fused the results of three SVM classifiers to increase the rate of the prediction. They extracted three groups of features, each of which was the input data of one classifier. For the first classifier, the features were the spatial coordinate values of the tooth contours. The second classifier run with the Fourier descriptors of the contours and the features of the third one were various geometrical tooth features such as the length of the tooth. The teeth were labelled by the Markov Chain Model which was based on the spatial relationships between the teeth. This system is very similar to ours because of using the SVM for classification and the graphical modelling for the labeling purposes. However, the features which are based on the tooth contours are not as robust as the candidates extracted by the filters used in our system, due to the fact that it is very hard to extract the contours of the teeth exactly in the radiographic images. Mahoor and Abdel-mottaleb (Mahoor and Abdel-mottaleb, 2005) presented a tooth classification and numbering system whose approach resembled the studies of the previous ones while instead of the SVM, they used the Bayesian function as the classifier with the Fourier descriptors of the extracted contours. The similar system of Frejlichowski and Wanat (Frejlichowski and Wanat, 2011b) differed from the previous ones such that they used a fitness function for tooth detection in the orthopantomograms. They first employed the watershed method to segment the images into the small fragments and then the fitness function determined whether a fragment belongs to a tooth or not based on the features related to the fragment.

The systems which use the panoramic images suffer from the teeth overlapping problem due to the technique to produce a panoramic image, the image stitching. Lira et al. (Lira et al., 2013) handled this common issue in their system. They initially reduced the noise in the images via the Gaussian filter and enhanced the images using the top-hat and the bottom-hat morphological operations. Then the Otsu thresholding method was applied to segment the teeth from the background and the candidate teeth were labelled. Afterwards, they applied the erode operation to find the seeds of the teeth. These seeds were used as masker points in the distance field which were produced by the distance transform operator and flood by the watershed algorithm. Next, the AND operator was applied between the generated mask and the Otsu result to detect the candidate teeth. Finally, the small regions were recovered using the close operation to eliminate the over-segmentation problem.

In addition to the systems which are applicable to the radiographs, there also exist several studies for the Computed Tomography (CT) and the Cone Bean Computed Tomography (CBCT) data. Kainmueller et al. (Kainmueller et al., 2012) used the Statistical Shape Model (SSM) in their method to split the jaws. They used the SSM for extracting the region containing the rows of the teeth. Then, the region was divided into the subregions such that each subregion contains only one row or its corresponding gap. The separation process was accepted as a discrete optimization problem and was solved using the Dijkstra's algorithm. After the segmentation step, the classifiers based on AdaBoost.M1 and Support Vector Machines run to determine whether the subregion contains a tooth or not. The classifiers used the intensity histograms of the subregions as the features. Gao and Chae (Gao and Chae, 2010) employed arch curve fitting on the CT images to split the jaws and integral intensity projection to isolate the individual teeth.

CHAPTER 3

THE TOOTH IDENTIFICATION FRAMEWORK

In an adult mouth, there should exist 32 teeth and they are divided into 4 classes: incisors, canines, premolars, and molars. In this study, the teeth on a jaw are represented as a set $t = \{t_1^j, t_2^j, \dots, t_{16}^j\}$ where t_i^j is a tooth label on the jaw $j \in \{upper, lower\}$. Since a panoramic dental radiograph, the image type used as input in this study, involves the whole mouth, there are 32 teeth in these images if there are not any missing teeth. However, in this thesis, the proposed system handles the canines with the incisors; therefore, there are 3 tooth classes instead of 4.

At the tooth detection stage, we divide the panoramic radiograph into 10 regions, each of which corresponds to one tooth set. As a result, on each jaw, 5 tooth sets are used for tooth detection where $t_m^r = \{t_6^j, t_7^j, t_8^j\}$ are the molar teeth on the right side of the jaw j, $t_m^l = \{t_{-6}^j, t_{-7}^j, t_{-8}^j\}$ are the molar teeth on the left side of the jaw j, $t_{pm}^r = \{t_4^j, t_5^j\}$ are the premolar teeth on the right side of the jaw j, $t_{pm}^l = \{t_{-4}^j, t_{-5}^j\}$ are the premolar teeth on the left side of the jaw j, $t_i = \{t_1^j, t_2^j, t_3^j, t_{-1}^j, t_{-2}^j, t_{-3}^j\}$ are the incisors and canine teeth of the jaw j. As a result the set of tooth sets on a jaw is represented by $t_s = \{t_m^r, t_m^l, t_{pm}^r, t_{pm}^l, t_i\}$ at this stage (Figure 3.1).

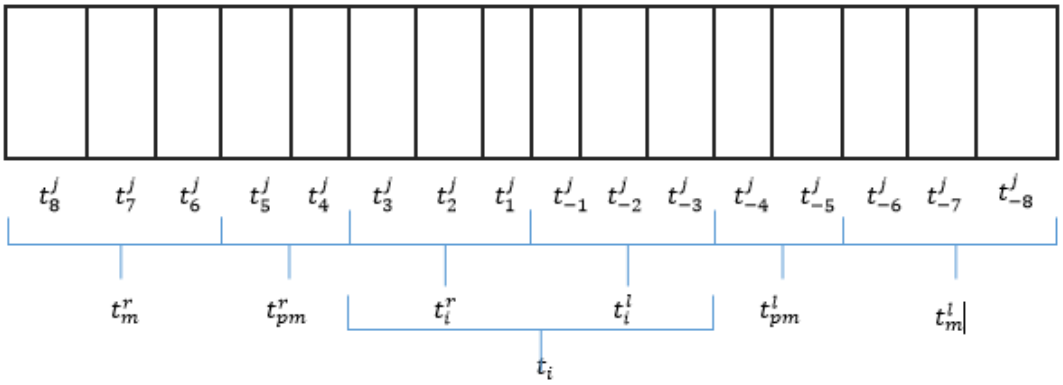

Figure 3.1 The tooth sets of a jaw.

Since the teeth in the t_i have low angular deviation from the nose position and therefore, their horizontal positions do not affect the feature extraction process significantly, we didn't divide this tooth set horizontally. However, at the labelling stage, we also divide this set horizontally due to our numbering approach. So, the set of tooth sets is changed as $t_s = \{t_m^r, t_m^l, t_{pm}^r, t_{pm}^l, t_i^r, t_i^r\}$ where $t_i^r = \{t_1^j, t_2^j, t_3^j\}$ are the incisors and canine teeth on the right side of the jaw j and $t_i^l = \{t_{-1}^j, t_{-2}^j, t_{-3}^j\}$ are the left side of the jaw j similarly. As a result, instead of 5, we use 6 tooth sets for each jaw at this stage.

The proposed system consists of the detection and the labeling modules which handles each tooth set separately such that the teeth in a tooth set is detected by the former and the detected teeth are labeled by the later one. The detection module has two componets: the feature extraction and the classification. The feature extraction component use two filters for extracting the Haar and the HOG desriptors from the tooth sets in the the panoramic radiographs, while the SVM and the Boosting techniques are employed for tooth classification. The classifiers are firstly trained with the training tooth and background images, and then tested on the test images. Section 5 discusses the tooth detection module.

The labelling module performs labelling based on our specific graphical tooth modelling method which is developed taking the intersection of the mouth gap and the centers of the first incisors, on the lower and the upper jaws separately, in a panoramic

radiograph, and the probable tooth widths into account. The labelling module determine the tooth labels receiving the candidate tooth locations detected by the detection module as input. This module consists of the following components: are the graphical tooth model, the best candidates selection component, the best tooth model(s) selection component, the missing tooth determination component, and the labelled image factory component. Section 6 handles the labelling module in detail. Figure 3.2 introduces the framework developed for tooth detection and labeling.

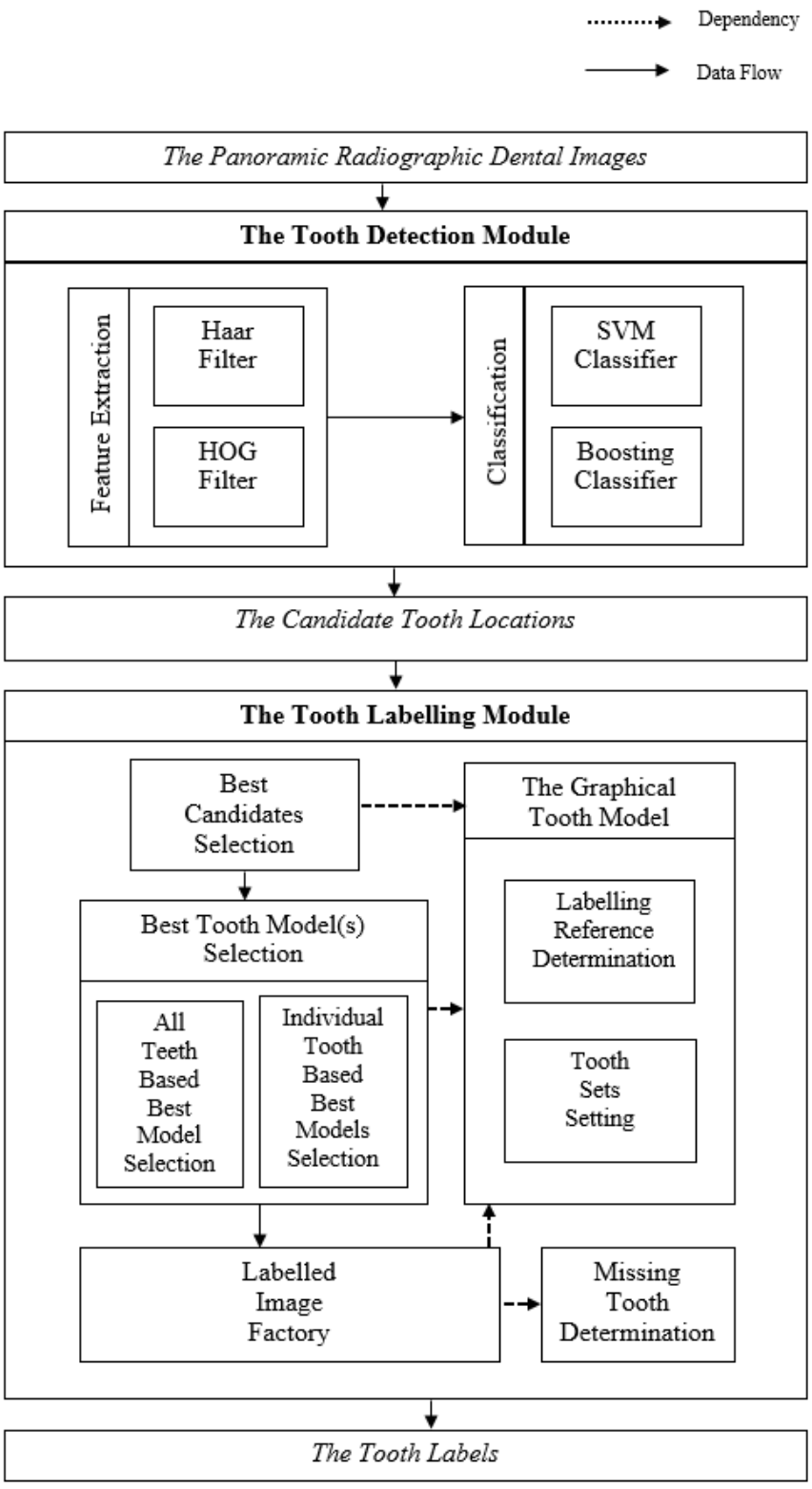

Figure 3.2 The framework consists of the tooth detection and labeling modules.

CHAPTER 4

THE TOOTH DETECTION MODULE

The main goal of the tooth detection module (Figure 4.1) in the proposed tooth idenfication framework is to produce candidate tooth locations for each tooth set which are taken as input by the tooth labeling module. The detection module has two main components: (i) Feature Extraction and (ii) Classification. The Feature Extraction module produces the input for the Classification module. The classifiers, based on the SVM and the Boosting algorithms, are firstly trained and then tested with the tooth sets in the panaromic radiographs for tooth classification. The Feature Extraction module uses the Haar and the HOG filters to extract the features of the teeth.

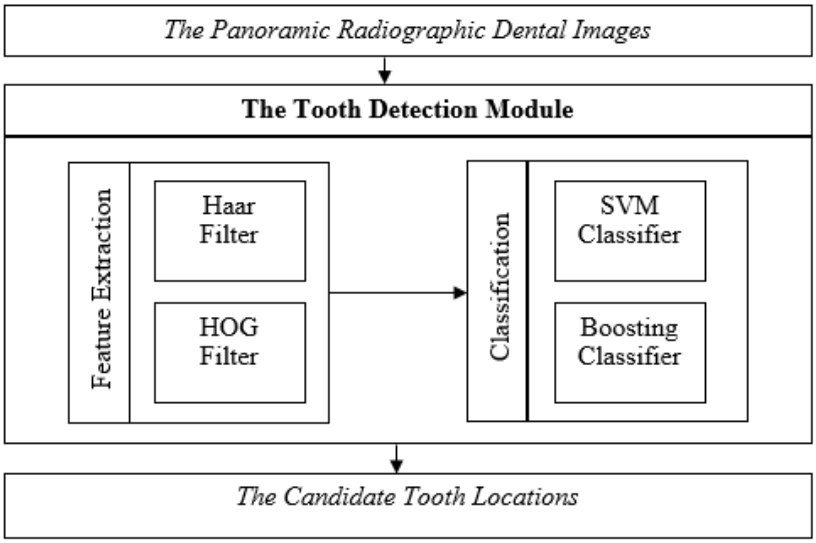

Figure 4.1 The Tooth Detection Module.

4.1 FEATURE EXTRACTION

An object is identified with its characteristics. In order to recognize it, an object is represented by its discriminative characteristics. These characteristics are called features and the process in which the features are found is called feature extraction.

The specialities of the search space, such as illumination and spatial properties, may affect the features of the object. Therefore, besides the distinctiveness, the features to be extracted should be invariant in the search space for effective object detection.

Considering all of these, in this thesis, the Haar and the HOG filters are used to extract the features of teeth in the panoramic radiographs. The main reason for preferring them is that, as the texture descriptors, instead of a single pixel intensity of a tooth, they take the whole structure of the tooth depending on the radiograph into account. As a result, the extracted features are more representative and firmer to the noise effect. This also provides to actualize the tooth detection process with fewer images (Viola and Jones, 2001).

4.1.1 Haar Filters

These features are similar to the Haar basis functions (Papageorgiou et al., 1998). They are grouped as two-rectangle, three-rectangle and four-rectangle features in the literature (Figure 4.2). The rectangles in a feature have the same size and shape, and are horizontally or vertically adjacent. A two-rectangle feature is the difference between the sum of the pixels within two rectangular regions. A three-rectangle feature subtracts the sum in the two outside rectangles from the sum in the center rectangle. A four-rectangle feature computes the difference between diagonal pairs of rectangles (Viola and Jones, 2001).

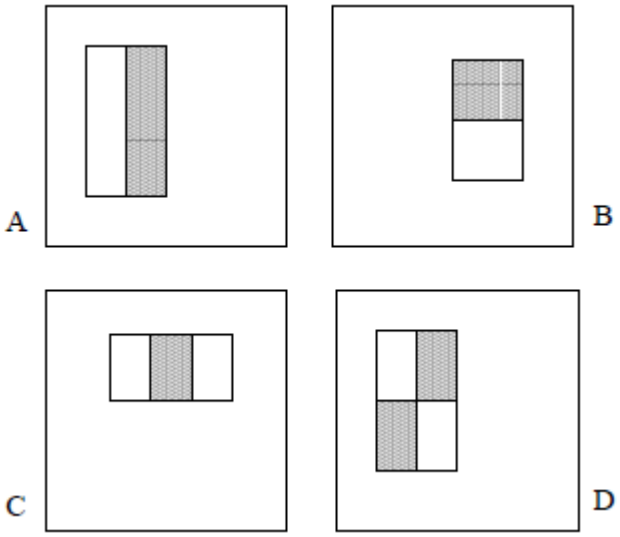

Figure 4.2 Haar filters (Viola and Jones, 2001).

4.1.2 HOG Filters

HOG features represent the distribution of local intensity gradients and edge directions. Instead of using edge positions or gradients themselves, these are preferred due to the fact that they give more accurate results than the former ones, even with the lack of exact pixel intensity values. A HOG feature is an enhanced representation of a special region within an image window. This special region is, called as block, constructed by smaller regions called cells. To compute a normalized block description, first of all, gradients are calculated for pixels in a cell. For compensating nonlinearity, features are determined based on orientation histograms constructed by channels. Each channel, also called bin, represents an interval for gradient orientation degrees between 0-360 for signed and 0-180 for unsigned gradients. To create this orientation histogram over cell, the gradient itself or one of its functions is used. This gradient related value is called vote. The accumulated votes in orientation bins produce the orientation histogram for each cell. The combined histogram entries form the final representation of the HOG features. In order to get the illumination invariant features, it is required to normalize neither the blocks or cells. This may be done by contrast normalization based on the blocks. So the final descriptor includes vectors of normalized cell values from all blocks (Figure4.3)(Seemann,2008).

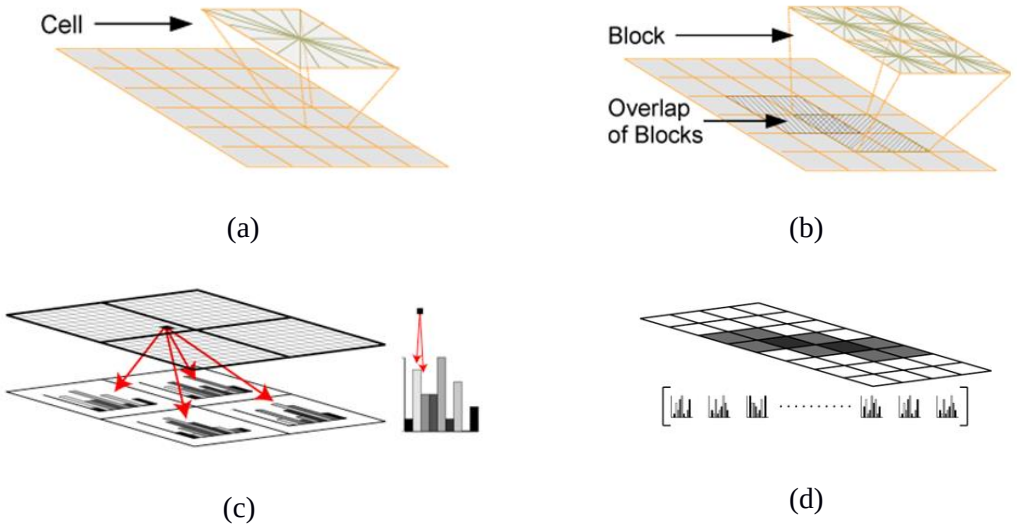

Figure 4.3 The components of the HOG filter: (a) cell, (b) block constructed by four cells, (c) orientation histogram of a cell constructed by bins, (d) concetanation of blocks (Seemann, 2008).

The orientation histograms may be divided into two classes according to their geometries. If the cells in a block are rectangular, the arrangement is called R-HOG, while they are circular, it is called C-HOG (Figure 4.4). A C-HOG may has a single or an angular partitioned central cell. In this thesis, the former one is used; because, they give the same performance despite having fewer cells. There are various normalization schemes for the geometries mentioned above, such as L2 Norm, L2-Hys, L1 Norm and L1-sqrt. (Dalal and Triggs, 2005).

(a) (b)

Figure 4.4 C-HOG filters: (a) C-HOG with a single circular central cell, (b) C-HOG whose central cell is divided into four angular sectors (Dalal and Triggs, 2005).

4.2 CLASSIFICATION

The classification module of the proposed system uses the supervised machine learning approach to classify a tooth as a molar, a premolar or an incisor. Two classification algorithms are utilized in this system: (i) Support Vector Machines and (ii) Boosting.

4.2.1 Support Vector Machines

A Support Vector Machine (SVM) (Welling, 2005) is a binary classifier. The main purpose of this learning algorithm is to find “the best” hyperplane which seperates the input data into two classes. The more distant the different data are, the easier it is to classify them; for that reason, it is wanted to find the maximum distance between two nearest samples which are in different classes. So, SVM tries to find the hyperplane, the best hyperplane, which provides the requirement above. It means that the best hyperplane locates at the middle of the distance between these samples. These reference samples which determines the best hyperplane are what are called support vectors and the distance between them is called margin (Figure 4.5).

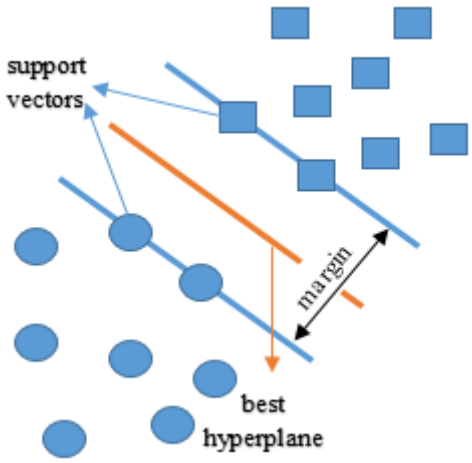

Figure 4.5 Support vectors determining the best hyperplane.

If the data distribution is linear, then the hyperplane can be represented by a linear function as $ax + by = c$. If the best hyperplane (H) is defined as $wx_i + b \geq +1$ when $y_i = +1$ and $wx_i + b \leq -1$ when $y_i = -1$, the planes on which the support vectors are located (H_1 and H_2) are formulated as $wx_i + b = +1$ and $wx_i + b = -1$ and from the formula of the distance between a point and a line, the distance between a support vector and the hyperplane is formulated as $2/\|w\|$ what is expected to maximize for finding the best hyperplane. As a result, the goal is to minimize $\|w\|$ such that boundary constrain is obeyed. So, the problem is handled as a constrained optimization problem and is solved by Lagrangian multiplier method (Berwick and Idiot, 2003).

If the data distribution is complex and nonlinear, then the hyperplane is formulated as a nonlinear function. Instead of making the separation using a nonlinear function, it is more appropriate to change the data space on which the hyperplane is formulated by a linear function. With this nonlinear function, the input data are moved to a higher dimensional space what is called feature space. On this space, again, the data are separated with a linear hyperplane (Figure 4.6).

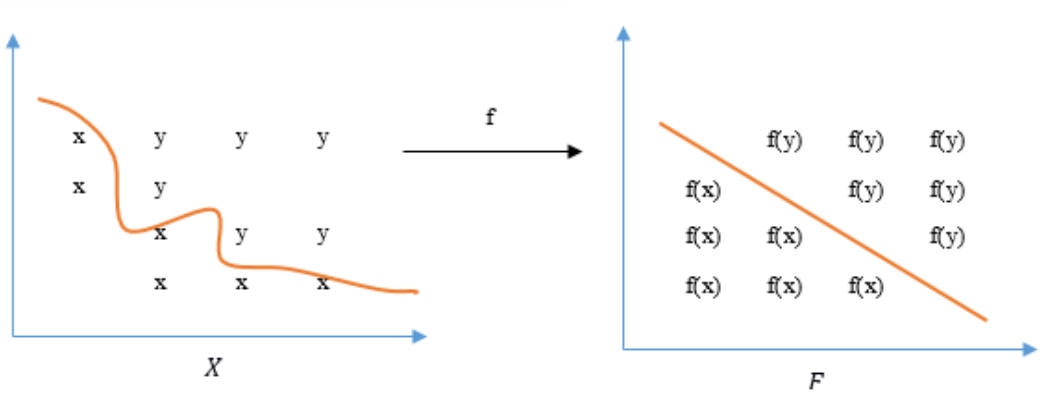

Figure 4.6 Transformation from input data space (X) to a higher dimensional feature space (F) using a nonlinear function (f).

For transforming the data distribution to a higher space, instead of using a nonlinear function as a transformation function, the dot products in Lagrangian multiplier formulas are converted to kernel functions. The kernels are the functions which give the same result with the dot products in a quicker way.

There are different types of kernels used in SVM such as polynomial kernel, Radial Basis Function (RBF) and Gaussian RBF Kernel (Stanevski and Tsvetkov, 2005).

4.2.2 Boosting

Boosting is a technique which enhances any learning algorithm's prediction ability. In the boosting strategy, the main idea is to establish a complex classifer constructed by simpler classifiers due to the fact that it is hard to find a function to be able to classify all the data accurately at once. Starting with a very weak classifier which is only silightly better than a random predictor, the classifer is improved by setting the dataset as increasing the weights of missclassifed samples and decreasing the weights of the samples classified accurately. So, the improved classifer will focus on the 'hard' samples. This learner strengthening process is repeated many times to construct a final strong learner which is a weighted combination of weak learners. Each weak learner's contribution weight is set according to the prediction error of this learner

(Schapire, 2002). The algorithm (Bouzy, 2013) below is sum marized the boosting strategy:

The Steps of The Boosting Algorithm

Input: Training Data $= \{(x_1\ ,\ y_1), \dots, (x_m\ ,\ y_m)\}$ where $x_i\ \in X,\ y_i\ \in \{-1, +1\}$

Repeating Number: t

Initial weight of an example in the training: $D_t\ (i) = 1/m$ where $\ t = 1,\ i = 1$

Interim outputs (for each round t*):* The weak learner at time t: h_t

Final output: The strong classifer (Figure 4.7)

1. Compute ε_t, the error of a weak hypothesis(classifier) h_t :

$$\varepsilon_t = Proba_{i\ in\ D_t}[h_t(x_i) \neq\ y_i] = \sum_{i:h_t\ (x_i)\neq y_i} D_t\ (i). \quad (4.1)$$

2. Compute $\propto_t$, the contribution value of the weak classifier h_t to the final strong classifier :

$$\propto_t = \frac{1}{2} ln\big((1 - \varepsilon_t)/\varepsilon_t\big) \quad (4.2)$$

3. Update the weights of the examples in the training data set based on the error rate to get the next weighted training data set such that if the sample is predicted accurately, decrease its weight and if the sample is not able to be predicted, its weight is increased :

$$D_{t+1}(i) =\ (D_t(i)/Z_t)\ exp(-\propto_t)\ if\ h_t(x_i) = y_i. \quad (4.3)$$

$$=\ (D_t(i)/Z_t)\ exp(+\propto_t)\ if\ h_t(x_i) \neq y_i$$

$(Z_t: normalization\ factor\ over\ i.)$.

4. Get weighted summation of all the weak classifiers h_t to get the final strong classifier *H:*

$$H(x) = sign\ \left(\sum_{t=1,\dots,T} \propto_t h_t(x)\right) \quad (4.4)$$

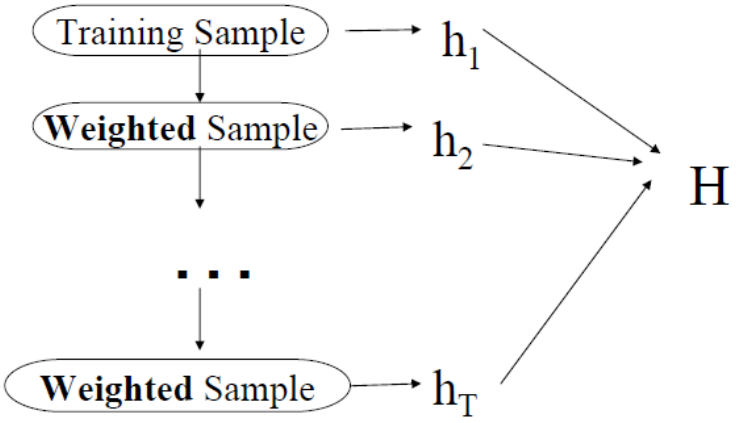

Figure 4.7 The boosting process to construct a strong classfier from weak classifiers (Bouzy, 2013).

There exists various Boosting algorithms which especially differ due to the methods of weighting training samples and weak classifiers. The most known is Adaboost which is the first method applied to the weak classifiers. LPBoost, TotalBoost, BrownBoost, MadaBoost and LogitBoost are some other examples of boostingmethods(Kumar,2012).

CHAPTER 5

THE TOOTH LABELLING MODULE

The tooth labeling module, the second module of the proposed tooth identification system, aims to identify each tooth in a panoramic radiographic dental image. This module takes the ouput of the tooth detection module, the candidate tooth locations, as input and produces the corresponding tooth labels in the labelling module as output.

5.1 THE LABELLING APPROACH

An In order to label the teeth, we use the graphical modelling approach with the statistical optimization techniques and the dynamic programming such that the labelling module produces the set of tooth models which are established based on the the graphical modelling and find the best model which resembles the pattern in the image the most using the dynamic programming and the optimization.

5.1.1 The Graphical Tooth Model

Let, $direction\ (d) = \{right, left\}$ and $jaw\ (j) = \{\ upper, lower\}$, in the proposed system, the teeth in the each quadrant of the panoramic image $t_d^j(c, w) = \left\{t_m^{dj}, t_{pm}^{dj}, t_i^{dj}\right\}$, where c and w symbolize the center of the tooth and the width of the tooth, respectively, are represented by the pictorial structure-like graphical model (Felzenszwalb and Huttenlocher, 2005) based on the undirected graph $G_d^j = \left(V_d^j, E_d^j\right)$

where the vertex V_d^j corresponds to the center of the tooth c_d^j, and the edge E_d^j corresponds the width based distance of the tooth w_d^j (see Figure 5.1).

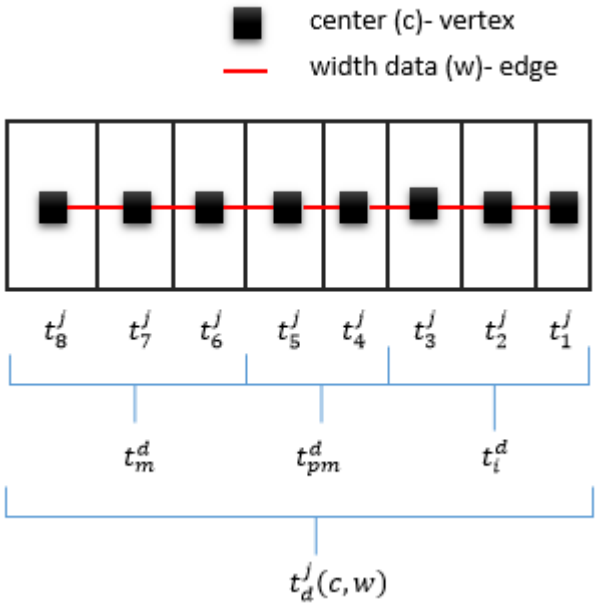

Figure 5.1 The proposed graphical tooth model for the right upper jaw.

Let the candidate tooth locations be represented by $l_d^j = \{l_1, \ldots, l_n\}$, according to the proposed approach, the set of the graphical models per image G_d^j are produced based on the variable structures, namely the teeth having variant widths and the mouth gaps, in the panaromic radiography and it is tried to find the best tooth model $G^* \in G_d^j$ for each tooth $t \in t_d^j$ or for all the teeth t_d^j in the search space based on the resemblance between the model and the pattern of the image, represented by l_d^j. The resemblance is measured by computing the differences between the tooth centers c_d^j and the corresponding candidates l_d^j.

5.1.2 The Labelling

In advance of comparing the tooth models for finding the best one, we, first, eliminate the inappropriate candidate tooth locations $l_{n-k} \in l_d^j$ according to the corresponding search space in the tooth models. After that, the appropriate candidates $l_k \in l_d^j$ are labelled for each tooh model. Let the cost $g_c(l_k)$ represents the distance of the candidate tooth location to the corresponding tooth center, the candidate $l_k \in l_d^j$ which is the closest one to the center of the corresponding tooth in the model, namely whose $g_c(l_k)$ is the minimum, is selected as the best candidate l_k^* of the same labelled candidates $l_k \in l_d^j$. While computing the proximity of the candidates l_k according to the tooth centers $c_k \in c_d^j$, the horizontal position of the candidate is also taken into account such that, it is desired to approximate the candidates each other while adapting them to the tooth model by trying to locate them into the centers of the tooth. This approach aims to provide the structure of the model by equalizing the opposite forces effecting the candidates (see Figure 5.2).

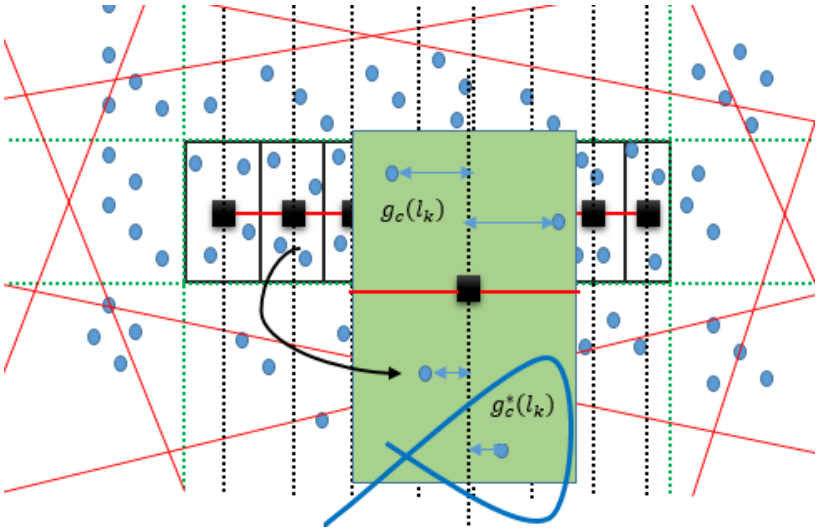

Figure 5.2 The best candidate tooth label selection where the empty black rectangle represents the tooth in the model (zoomed version is the green filled rectagle), the black filled rectangle is the center of the tooth in the model, the red line within the black rectangle respresents the half of the tooth width, the blue filled circles represent the candidate tooth locations, the regions marked by cross red lines represent the invalid regions according to the graphical model in which the candidates are eliminated, the blue arrowed line represents the distance of the candidate location to the tooth center, and the black and the green dashed lines are the reference lines.

We use two approaches to find the best tooth model G^* which is the most similar model to the pattern in the image represented by the candidate tooth location / locations $l_k \in l_d^j$ determined by the detection module. The first approach selects the unique best model for all the teeth t_d^j, and the second approach determines the best tooth model per tooth $t_k \in t_d^j$ in the search space. It means, the first approach searches the best model horizontally and the second approach searches the best model vertically considering the relations of the teeth and the tooth models. Therefore, in the following, the first approach is called as the horizontal approach (h-approach), and the second approach is called the vertical approach (v-approach) (see Figure 5.3).

	$t^{ru}_{m_3}$	$t^{ru}_{m_2}$	$t^{ru}_{m_1}$	$t^{ru}_{pm_2}$	$t^{ru}_{pm_1}$	$t^{ru}_{i_2}$	$t^{ru}_{i_1}$
G_1	$cost_1$	$cost_1$	$cost_1$	$cost_1$	$cost_1$	$cost_1$	$cost_1$
G_2	$cost_2$	$cost_2$	$cost_2$	$cost_2$	$cost_2$	$cost_2$	$cost_2$
G_3	$cost_3$	$cost_3$	$cost_3$	$cost_3$	$cost_3$	$cost_3$	$cost_3$
G_4	$cost_4$	$cost_4$	$cost_4$	$cost_4$	$cost_4$	$cost_4$	$cost_4$
G_5	$cost_5$	$cost_5$	$cost_5$	$cost_5$	$cost_5$	$cost_5$	$cost_5$
G_6	$cost_6$	$cost_6$	$cost_6$	$cost_6$	$cost_6$	$cost_6$	$cost_6$

Figure 5.3 The h-approch and the v-approach for best tooth model selection.

We use two methods for selecting the best tooth model G^* and/or models $G_d^j *$ which differ in establishing the relationships between the teeth t_d^j in the graphical model. Namely, we use two types of cost functions each of which represents the dissimilarity between the image and the tooth model $G_x \in G_d^j$ such that the tooth model which minimizes the cost function the most is selected by the best tooth model G^*.

Let $dist_{opt}(c_{k-1}, k)$ represents the distance between the centers of the adjacent teeth as the optimum distance and $dist_{act}(l_{k-1}, l_k)$ represents the distance between the adjacent candidate tooth locations as the actual distance, then, in our first method, we find the tooth cost $cost(t_k)$ as the difference between the optimum and the actual distance. Because of considering the distances of the adjacent teeth, we call this cost as the binary cost (bi-cost) which is formulated as

$$bi - cost(t_k) = \left|dist_{opt}(c_{k-1}, c_k) - dist_{act}(l_{k-1}, l_k)\right| \quad (5.1)$$

where $dist_{opt}$ represents the optimum distance and $dist_{act}$ represents the actual distances mentioned above (see Figure 5.4).

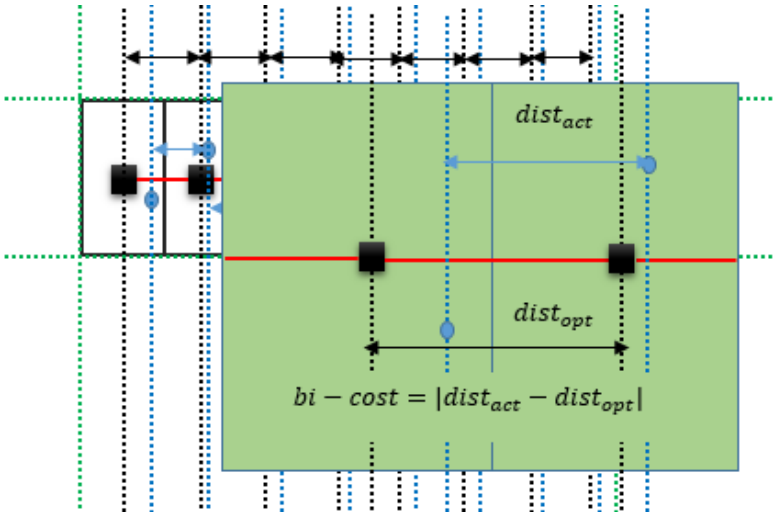

Figure 5.4 The bi-cost computation where the empty black rectangle represents the tooth (zoomed version is the green filled rectangle), the black rectangle is the tooth center, the red line is the half of the tooth width, the black arrowed line represents the optimum distance (the distance between the centers of the two adjacent teeth), the blue arrowed line represents the actual distance (the distance between the adjacent best tooth candidates for the adjacent teeth), and the black and the green dashed lines are the reference lines.

On the other hand, the second method, first, computes the distance between the center of the tooth and the center of the first incisor as the optimum distance represented by $dist_{opt}(c_k, c_f)$ for the tooth t_k, and the distance between the candidate tooth and the end of the search space as the actual distance represented by $dist_{act}(l_k, main\ ref\ (r))$. In order to compute the tooth cost, the difference between the actual distances of the adjacent teeth is subtracted from the difference between the optimum distances of the adjacent teeth. This cost is called as the distant cost (d-cost) due to measuring the distancing from the initial point and formulated by

$$d - cost(t_k) = \left|dist_{opt}\left(c_{(k-1)f}, c_{kf}\right) - dist_{act}(l_{(k-1)r}, l_{kr})\right| \quad (5.2)$$

where $dist_{opt}$ represents the optimum distance and $dist_{act}$ represents the actual distances mentioned above (Figure 5.5).

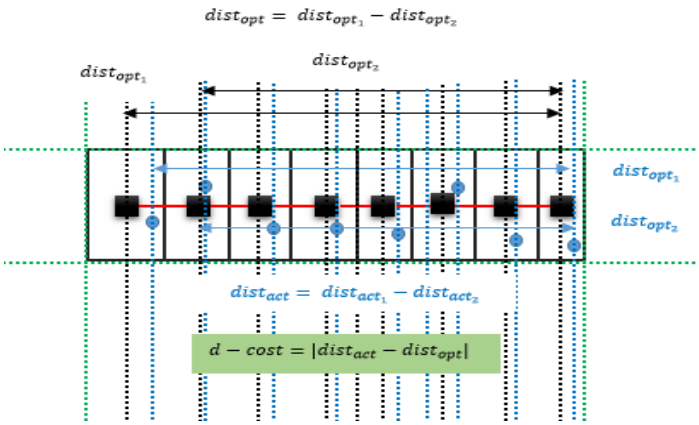

Figure 5.5 The d-cost computation where the empty black rectangle represents the tooth in the model, the black filled rectangle represents the tooth center, the red line within the tooth represents the half of the tooth width, the blue filled circles are the candidate tooth locations, the blue arrowed line represents the distance between the first incisor and the candidate, the black arrowed line represents the distance between the tooth center and the center of the first incisor, and the black and the green dashed lines are the reference lines.

The following procedures are the same for the both methods: The procedure of computing the $cost(t_k)$ is repeated for all the teeth $t_k \in t_d^j$ and for all the tooth models $G_x \in G_d^j$. The tooth costs are summed up horizontally to find the best model for the h-approach, and vertically to find the best models for the v-approach using the Eqs. (5.3) and (5.4). The algorithm of the proposed labelling module is presented below.

The Steps of The Labelling Algorithm

Input: Candidate tooth locaions $l_d^j = \{l_1, \dots, l_n\}$ where $d = \{right, left\}$ and $j = \{upper\ jaw, lower\ jaw\}$

Output: The tooth labels

For each jaw j;

1. Set tooth widths for each tooth set $t_d^j = \{t_m^{dj}, t_{pm}^{dj}, t_i^{dj}\}$ from minimum to maximum tooth width values, and the mean value (6 values in total).

2. Determine the intersection point of the first incisors and the mouth gap, called the main reference.

3. Determine the search space vertical border lines.

(*Based on the information obtained at the end of the steps above, the tooth models are constructed intuitevly.)*

For each horizontal side d of the jaw ;

4. Compute the horizontal distances of each candidate to the main referecence point.

For each tooth model;

5. Determine the label l_k for each candidate according to the distance and the width of the tooth in the tooth model which corresponds to the candidate.

6. Find the best candidate l_k^* within the same labelled candidates such that it provides the minimum cost $g^*(l_k^*)$ which represents the minimum distance to the center of the corresponding tooth in the model. However, take the horizontal side of the candidate relative to the tooh center into account first such that if the corresponding tooth is not the first incisor, search the side which is closer to the main reference first if there exist a detected candidate within it or not, then, search the the other side whether it does not. If the corresponding tooth is the first incisor, search the candidates in the opposite order.

(At this point, the best labels for each tooth set are determined. In the following, it is aimed to select the best tooth model.)

7. For each tooth t_k, compute the $bi-cost$ of the adjacent teeth which represents the absolute difference between the optimum distance $dist_{opt}$, the distance between the adjacent tooth centers c_{k-1} and c_k, and the actual distance $dist_{act}$, the distance between the adjacent candidate locations l_{k-1} and l_k ;

$$bi-cost(t_k) = \left|dist_{opt}(c_{k-1}, c_k) - dist_{act}(l_{k-1}, l_k)\right| \tag{5.1}$$

8. For each tooth t_k, compute the optimum distance which represents the distance of the tooth to the the center of the first incisor and actual distance which represents the distance between the main reference and the tooth. Then, compute the $d-cost$ of the adjacent teeth which represents the absolute difference between the $dist_{opt}$, the difference of the distances between the optimum distances of the adjacent teeth, and the $dist_{act}$, the difference of the actual distances between the adjacent djacent teeth ;

$$d-cost(t_k) = \left|dist_{opt}\left(c_{(k-1)f}, c_{kf}\right) - dist_{act}(l_{(k-1)r}, l_{kr})\right| \tag{5.2}$$

9. For both of the methods in **8.** and **9.** , apply the h-approach separately to select the best tooth model; Find the best tooth model G^* which minimizes the total cost, the summation of all the tooth costs;

$$cost(G^*)_d^{j^*} = \arg\min_{cost_d^j}\Big(\quad \sum_{j=1}^{n-1} cost_{ij}(G_k)\Big)$$

(5.3)

10. For both of the methods in **8.** and **9.** , apply the v-approach separately to select the best tooth models for each tooth;

$$cost(t^*)_d^{j^*} = \arg\min_{cost_d^j}\Big(\quad \sum_{j=1}^{n-1} cost_{ij}(t_k)\Big)$$

(5.4)

11. Compute the mean intensity of the mouth gap by looking a small region around the main reference. Compute the mean intensity of the detected teeth by applying the same method for each detected tooth and taking the mean of the values. Determine the mean intensity of the detected candidate using the same approach and decide if the candidate is located at the missing tooth position or not by calculating the proximity of the intensity values; If the mean intensity calculated for the candidate is closer to the one of the mouth gap, it represents the missing tooth, else not.

12. Combine all the results.

13. Produce all the labels based on the selected model / models, taking the missing tooth derermination into account.

5.2 THE COMPONENTS OF THE MODEL

The labelling components involved by the tooth labelling module are the graphical tooth model, the best candidates selection component, the best tooth model(s) selection component, the missing tooth determination component, and the labelled image factory component (Figure 5.7). The graphical tooth modelling component is the model which establishes the series of tooth models each of which is constructed based on the variable tooth widths and the intersection points of the mouth gap and the center of the first incisors as the base reference point. The best candidate for a tooth is determined by the best candidate selection component according to the distance of the candidate to the corresponding tooth's center in the tooth model. The best candidates for

all teeth are selected separately for each tooth model in the tooth models series presented by the graphical modelling component. The selection of the unique best tooth set for all the teeth or the best tooth sets for the individual teeth is performed by the best tooth model and/or models selection component such that the total difference or the differences per tooth between the optimum locations of the candidates and their actual locations is minimized. After the selection of the tooth model and/or models, the labelled image factory component produces the image in which all the teeth are labelled according to the optimum locations of the selected best tooth model and/or models, taking the predictions of the missing tooth determination component into account. The missing tooth is determined by comparing the mean intensity of the particular region enclosed the candidate tooth with both the mouth gap color and the mean intensity of the labelled teeth such that the proximity of the intensities determine whether the candidate is located in the missing tooth location or not.

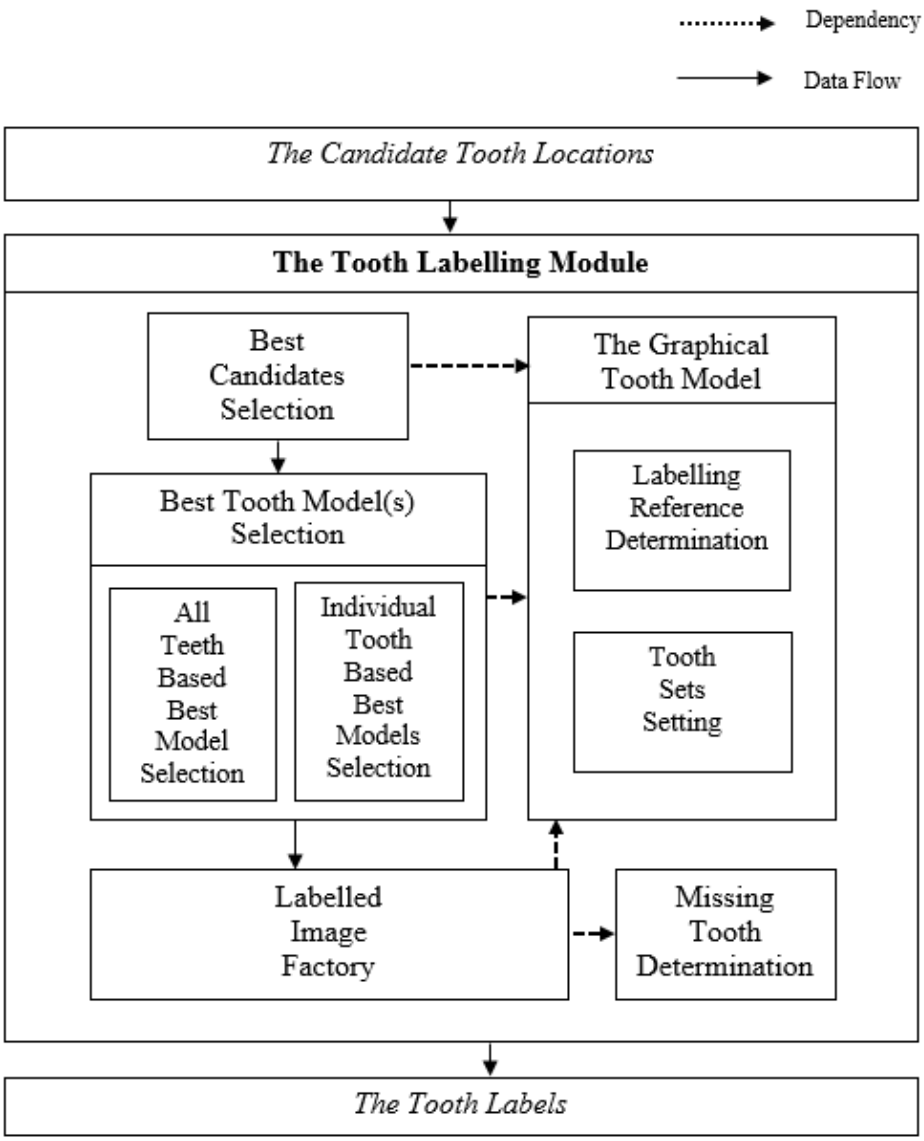

Figure 5.6 The Tooth Labelling Module.

CHAPTER 6

THE EXPERIMENTAL RESULTS

We use the panoramic dental radiographic dataset supplied by the Dental Hospital of the Kocaeli University in every implementation stage of the proposed tooth identification system. The images in the dataset belongs to the people older than 18. The dataset involve the missing teeth, dental work and the implants. Figure 6.1 shows a sample panoramic image from the dataset.

Figure 6.1 A panoramic radiograph from the dataset used in the system.

The software of the system is written in C++ language by using the Microsoft Visual Studio 2010 as the editor. In the following, the implementation is discussed step bystep.

6.1 THE EVALUATION OF THE TOOTH DETECTION MODULE

Our tooth detection module is established based on the supervised machine learning approach as mentioned above. It means, the initial step for detection is preparing the training set. The features which are given to the classifiers are extracted from these training data. After training of the classifiers, the trained classifiers perform the classification with the new features extracted from the 20 test images.

6.1.1 The Pre-processing

For training, 25-30 tooth and 50-60 background images for each tooth set are cropped from the radiographs manually. The reference coordinates of the tooth sets are computed, as the ground truth, based on the images in the dataset to divide the test images into the tooth sets automatically.

6.1.2 The Feature Extraction

The Haar and the HOG filters within the Open Computer Vision (OpenCV) library are utilized for the feature extraction. However, considering the performance, only the most distinctive features of the Haar filter are selected: 16x6, 16x32, 16x48, 16x64, 32x16, 32x32 horizontal and vertical two-rectangles; 48x16 horizontal three-rectangles; 16x48 vertical three-rectangles ; 16x16 and 16x32 four-rectangles. R-HOG filter, instead of the C-HOG, is preferred as the second descriptor due to its compatibility with the tooth structure. It is employed with 8x8 block constructed by 4x4 cells. Each cell is represented by the orientation histogram with 9 bins such that each bin corresponds to a particular value of the pixel gradient in the cell, between 0-180.

Initially the features are extracted from the training data to train the classifiers. Then the test images are divided into the tooth sets automatically based on the reference coordinates. The features for each tooth set are extracted using the sliding window technique on 20 different images in the testing step. Each sliding window is firstly accepted as a background image and the extracted features are marked as background features. The window size is between the minimum and the maximum size of the positive training images.

6.1.3 The Classification Module

For classification, the SMO and the AdaBoostM1 functions within the WEKA are integrated with our software as the SVM and the Boosting methods. These classifiers are firstly trained by the training features. Then, they classify the window which the features belong to, into a particular tooth or a background.

6.1.4 The Visual Detection Results

The detection module runs for each tooth set separately. Figure 6.2 and 6.3 shows the sample results of the detection module for Boosting and the SVM methods for the same dental radiograph respectively.

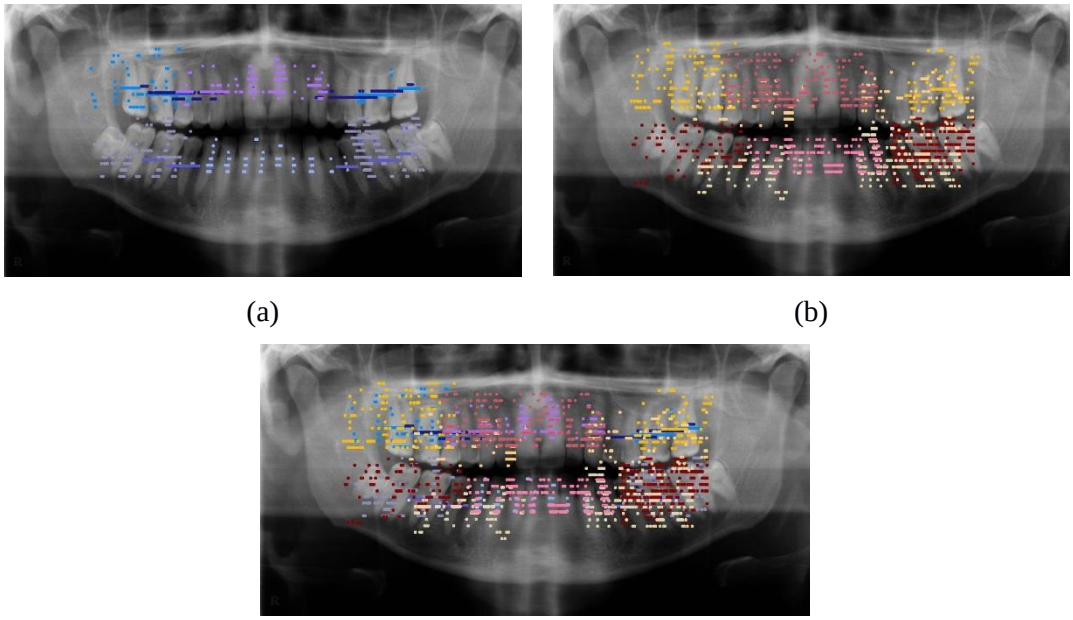

(a) (b)

(c)

Figure 6.2 The visual results of the detection module using the Boosting method where (a) shows the visual detection result of the Boosting with the Haar, (b) shows the visual detection result of the Boosting with the HOG, and (c) shows The visual detection result of the Boosting with the Haar and the HOG. Each color corresponds a different tooth class(molar/premolar/incisor).

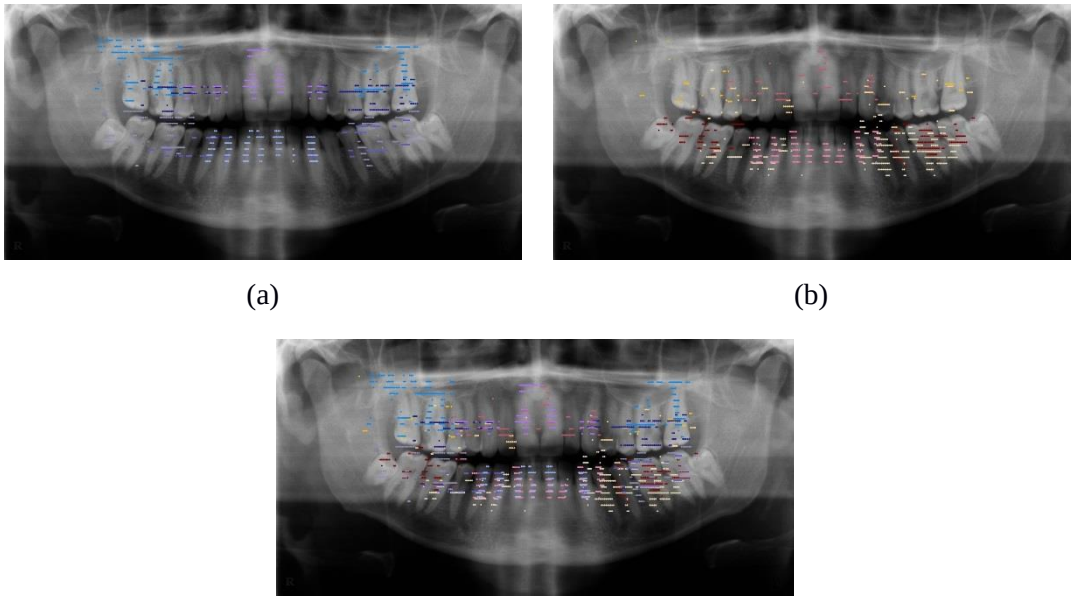

(a) (b)

(c)

Figure 6.3 The visual results of the detection module using the SVM method where (a) shows the visual detection result of the SVM with the Haar, (b) shows the visual detection result of the SVM with the HOG, and (c) shows The visual detection result of the SVM with the Haar and the HOG. Each color corresponds a different tooth class (molar / premolar / incisor).

6.1.5 The Numerical Detection Results

The detection module is evaluated using a specific metric which computes the rate of acceptable windows to all the predictions of the WEKA. The acceptability of a predicted window is determined according to the reference images in which the teeth are marked accurately. If a predicted window involves more than the half of the pixels of a corresponding tooth, this window is accepted as an accurate prediction; otherwise, not. The evaluation results are presented in Table 6.1 and Table 6.2.

Table 6.1 The numerical results of the detection module while using the SVM.

		HAAR				HOG			
		Upper Jaw		Lower Jaw		Upper Jaw		Lower Jaw	
		Right	Left	Right	Left	Right	Left	Right	Left
SVM	molar	0.62	0.79	0.53	0.72	0.48	0.72	0.59	0.85
	premolar	0.44	0.44	0.54	0.47	0.21	0.24	0.32	0.34
	incisor	0.71		0.51		0.59		0.67	

Table 6.2 The numerical results of the detection module while using the Boosting.

		HAAR				HOG			
		Upper Jaw		Lower Jaw		Upper Jaw		Lower Jaw	
		Right	Left	Right	Left	Right	Left	Right	Left
Boosting	molar	0.42	0.74	0.56	0.50	0.27	0.44	0.36	0.50
	premolar	0.33	0.39	0.43	0.30	0.12	0.14	0.21	0.20
	incisor	0.62		0.33		0.38		0.30	

6.1.6 The Discussion

The accuracy rate of the detection module is at most 85% for molars and at least 12% for premolars. The accuracy rates are low especially for some tooth classes as expected and it is caused by the similarity of teeth in the different tooth sets. Because the structure of the molars are very similar to the premolars, the neighboring molars are also detected as premolars. Since the molars has more features than premolars, the opposite is not valid. In addition, we skipped the image enhancement step due to the various and numerous corruptions in the panoramic images; more accurate results may be taken if the images are enhanced in advance of the detection. Furthermore, the extracted features may not representative enough to detect a particular tooth of a tooth set in a dental panaromic image. Despite of the fact that the results are raised by the labelling module, more robust features may be invented to get better results. It should be emphasized that the accuracy rate of the detection module does not show the success

of the proposed identification system; because, the aim of the detection module is not localization of the teeth accurately. This module only tries to find the candidate tooth locations which limit the search space for the labeling module.

6.2 THE EVALUATION OF THE TOOTH LABELLING MODULE

Since the accuracy rate of the detection module is higher while using the SVM as the classifer and the Haar descriptor as the feature extraction filter, the labelling is accomplished based on the output of the tooth detection with these two components.

6.2.1 The Pre-processing

In order to construct the tooth models with the optimum tooth width values, 20 images from the dataset are used to determine the minimum and the maximum width values. Table 6.3 shows the minimum and the maximum tooth widths used in the proposed system. The order is from the closest tooth to the furthest one.

Table 6.3 The minimum and the maximum tooth widths used in the tooth models.

	upper jaw		lower jaw	
	minimum	maximum	minimum	maximum
molar	{120,120,100}	{170,170,150}	{150,150,145}	{225,225,250}
premolar	{80,76}	{130,126}	{80,85}	{100,110}
incisor	{80,70,74}	{130,120,124}	{55,60,70}	{85,90,110}

In addition, it is required to determine the intersection point of the mouth gap and the center of the first incisors as the main reference to construct the tooth models. Our approach for this is similar to the one used by Wanat and Frejlichowski in their study (Wanat and Frejlichowski, 2011a) such that, first, the integral intensity projection is used vertically in a particular area surrounding the center of the image to determine the mouth gap, and then, the nose position is detected as the center of the first incisors using

the integral intensity projection horizontally in a certain region corresponding the probable nose position based on the detected mouth gap (Figure 6.4.a). The two approaches differ in the selection of the search regions. Because, in some of the images, this main reference determination is not successful (Figure 6.4.b), besides the automatic determination, this process is also performed manually in the proposed system to measure the exact accuracy rates of the proposed labelling methods. However, it is expected that the accuracy rate of the automatic main reference determination will increase if the images are enhanced beforehand and the system will become fully automatic while giving similar results with the ones when the manul determination is employed.

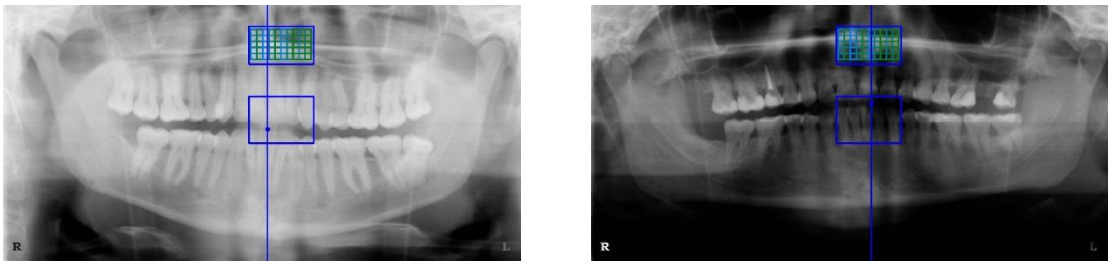

(a) (b)

Figure 6.4 The determination of the intersection point of the mouth gap and the nose position based on the integral intensity projection method where presents an acceptable result, the prediction in (b) is not accurate.

6.2.2 The Labelling Results

The test images are divided into the 4 quadrants and for each quadrant the labelling is performed based on the three tooth classes, namely, the molars, the premolars and the incisors including the canines. After obtaining the results per quadrant, they are combined and a single labelled image is produced. The labelling is implemented for both labelling methods, based on the bi-cost and the d-cost,

respectively, and for both approaches, the h-apprach and the v-approach, proposed in our sytem.

The following figures show the results when the main reference is determined manually (Figure 6.5-6.7).

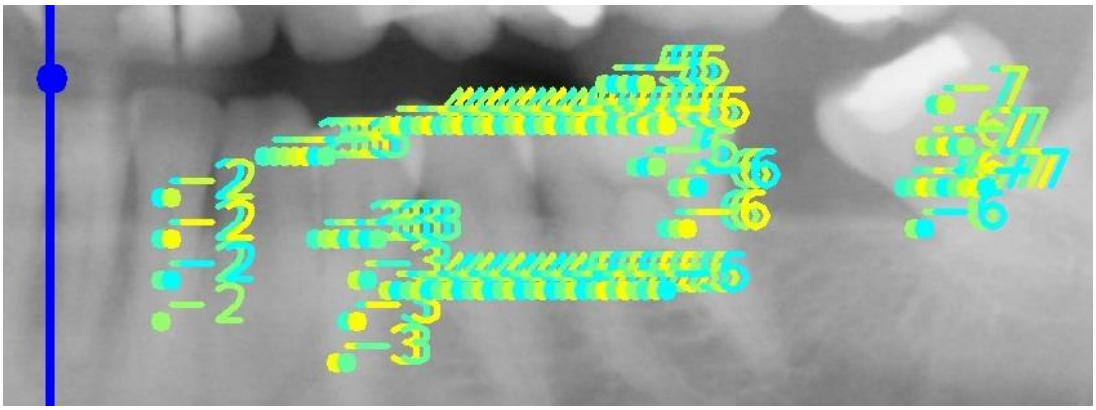

Figure 6.5 The visual result of the candidate labelling process for the left lower jaw.

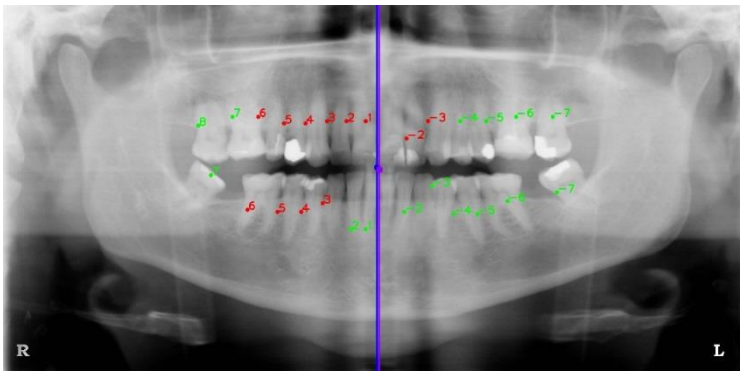

(a)

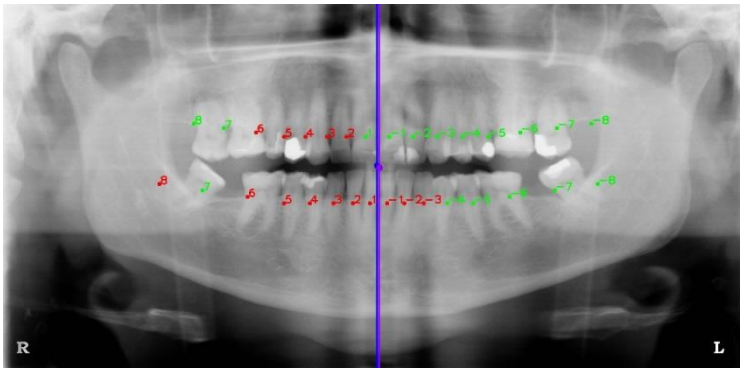

(b)

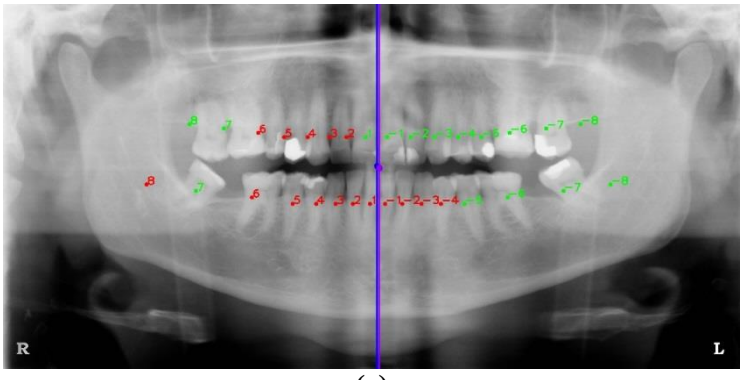

(c)

Figure 6.6 The visual results of the semi-automatic labelling method based on the bi-cost where (a) shows the combination of the selected best labels per quadrant from all tooth models, (b) shows the result of the produced labels for this method based on the h-approach and (c) shows the production results based on the v-approach.

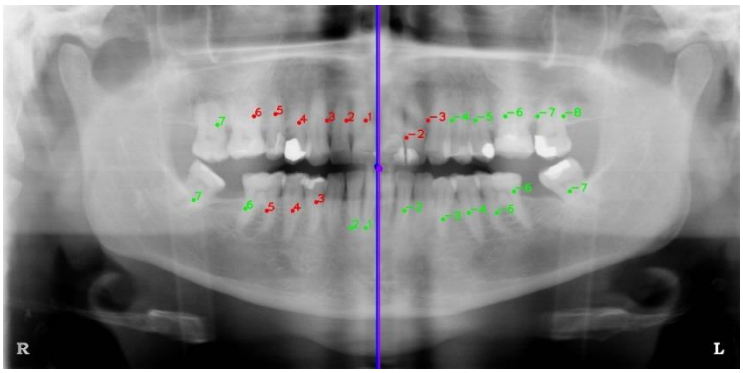

(a)

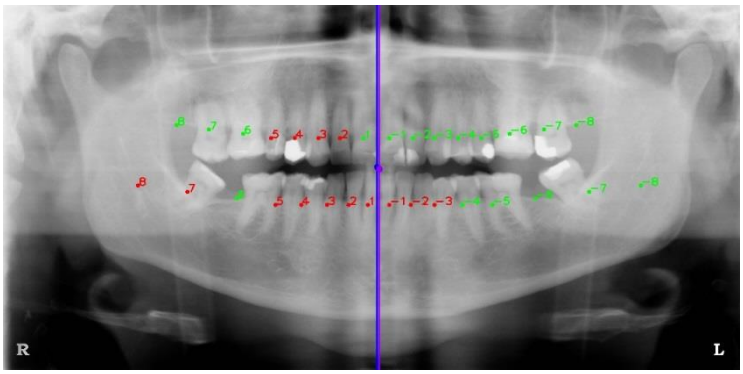

(b)

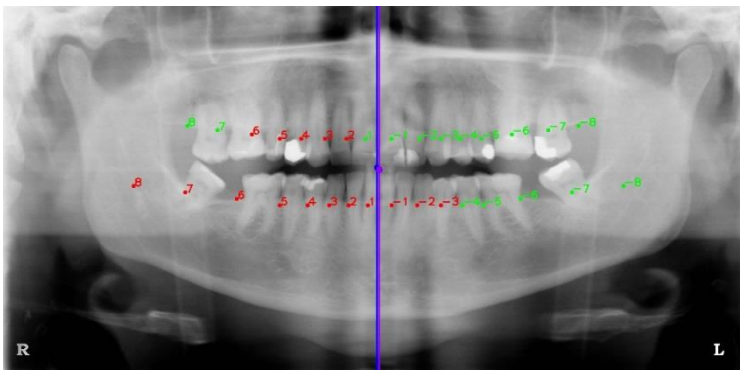

(c)

Figure 6.7 The visual results of the semi-automatic labelling method based on the d-cost where (a) shows the combination of the selected best labels per quadrant from all tooth models, (b) shows the result of the produced labels for this method based on the h-approach and (c) shows the production results based on the v-approach.

As seen the following figures, when the main reference is determined automatically, the success of the labelling methods decrease due to the fact that the models are constructed based on the main reference and even a slight movement may effect the labelling order in some degree. Figure 6.8 shows the results of the labelling

method based on the bi-cost while Figure 6.9 shows the same results if the method based on the d-cost is used when the main reference is determined automatically.

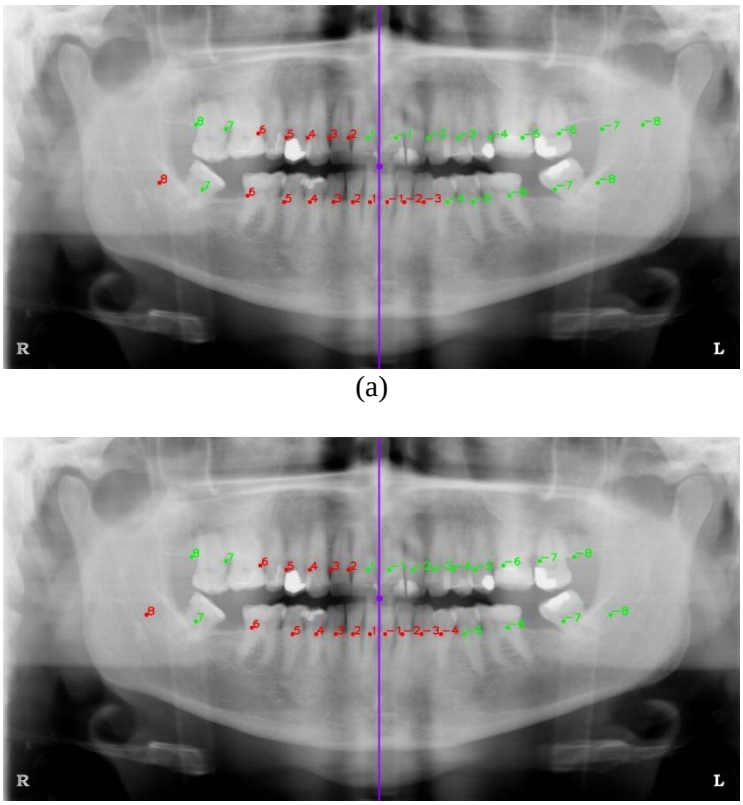

(a)

(b)

Figure 6.8 The visual results of the fully-automatic labelling method based on the bi-cost while using the h-approach (a) and v-approach (b).

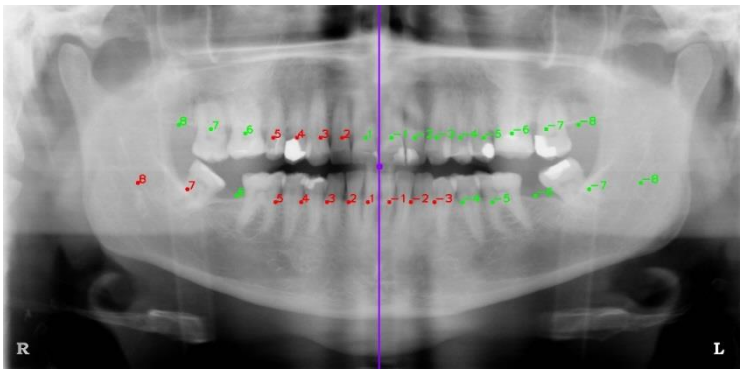

(a)

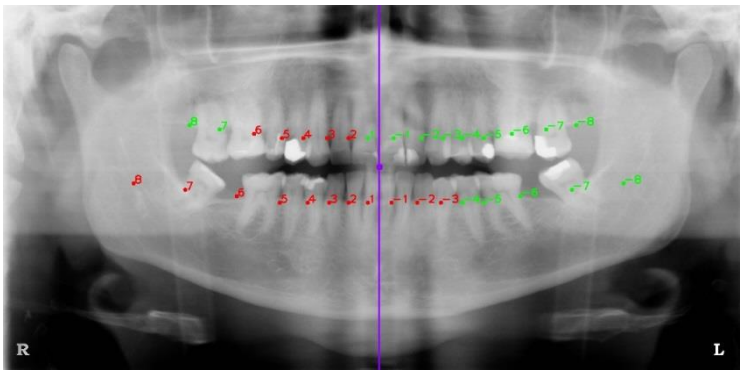

(b)

Figure 6.9 The visual results of the fully-automatic labelling method based on the d-cost while using the h-approach (a) and v-approach (b).

6.2.3 The Evaluation

We compute the rate of the accurate predictions to all the predictions as the accuracy metric, similar to the metric used in the detection module, per quadrant of the image to measure the success of the labelling module.

If the main reference is determined manually, when the labelling method based on the bi-cost is used with the h-approach, in the right side of the upper jaw, 102 out of 139 teeth, in the left side of the upper jaw 97 out of 140 teeth, in the right side of the lower jaw, 110 out of 147 teeth, and in the left side of the lower jaw 108 out of 141 teeth are labelled accurately. On the other hand, when the labelling method based on the bi-cost is used with the v-approach, in the right side of the upper jaw, 100 out of 139 teeth, in the left side of the upper jaw 96 out of 140 teeth, in the right side of the lower jaw, 126 out of 147 teeth, and in the left side of the lower jaw 110 out of 141 teeth are labelled

accurately. Table 6.4 shows the accuracy rates of the labelling method based on the bi-cost when the main reference is determined manually.

Table 6.4. The numerical results of the labelling based on the bi-cost when the main reference is determined manually.

	Upper Jaw		Lower Jaw			
	Right	Left	Right	Left	Total	
					Right	Left
h-approach	0,73	0,69	0,75	0,77	0,71	0,76
					0,74	
v-approach	0,72	0,69	0,86	0,78	0,70	0,82
					0,76	

When the labelling method based on the d-cost is used with the h-approach, in the right side of the upper jaw, 95 out of 139 teeth, in the left side of the upper jaw 79 out of 140 teeth, in the right side of the lower jaw, 87 out of 147 teeth, and in the left side of the lower jaw 111 out of 141 teeth are labelled accurately. On the other hand, when the labelling method based on the d-cost is used with the v-approach, in the right side of the upper jaw, 89 out of 139 teeth, in the left side of the upper jaw 100 out of 140 teeth, in the right side of the lower jaw, 102 out of 147 teeth, and in the left side of the lower jaw 99 out of 141 teeth are labelled accurately. Table 6.5 shows the accuracy rates of the labelling method based on the d-cost.

Table 6.5. The numerical results of the labelling based on the d-cost when the main reference is determined manually.

	Upper Jaw		Lower Jaw			
	Right	Left	Right	Left	Total	
					Right	Left
h-approach	0,68	0,56	0,59	0,80	0,62	0,70
					0,66	
v-approach	0,64	0,71	0,69	0,71	0,68	0,70
					0,69	

If the main reference is determined automatically, as stated above, the accuracy rate falls down: when the labelling method based on the bi-cost is used with the h-approach, in the right side of the upper jaw, 77 out of 139 teeth, in the left side of the upper jaw 78 out of 140 teeth, in the right side of the lower jaw, 89 out of 147 teeth, and in the left side of the lower jaw 74 out of 141 teeth are labelled accurately. On the other hand, when the labelling method based on the bi-cost is used with the v-approach, the results are closer to the results while determining the main reference manually: In the right side of the upper jaw, 103 out of 139 teeth, in the left side of the upper jaw 100 out of 140 teeth, in the right side of the lower jaw, 98 out of 147 teeth, and in the left side of the lower jaw 97 out of 141 teeth are labelled accurately (see Table 6.6).

Table 6.6. The numerical results of the labelling based on the bi-cost when the main reference is determined automatically.

	Upper Jaw		Lower Jaw			
	Right	Left	Right	Left	Total	
					Right	Left
h-approach	0,55	0,56	0,61	0,52	0,56	0,57
					0,57	
v-approach	0,74	0,71	0,67	0,69	0,73	0,68
					0,71	

The accuracy reduction degree of the d-cost based method is similar to the one of the previous method if the main reference is determined automatically, as expected: when the labelling method based on the d-cost is used with the h-approach, in the right side of the upper jaw, 85 out of 139 teeth, in the left side of the upper jaw 78 out of 140 teeth, in the right side of the lower jaw, 82 out of 147 teeth, and in the left side of the lower jaw 86 out of 141 teeth are labelled accurately. On the other hand, when the labelling method based on the d-cost is used with the v-approach, in the right side of the upper jaw, 89 out of 139 teeth, in the left side of the upper jaw 100 out of 140 teeth, in the right side of the lower jaw, 104 out of 147 teeth, and in the left side of the lower jaw 91 out of 141 teeth are labelled accurately (see Table 6.7).

Table 6.7. The numerical results of the labelling based on the d-cost when the main reference is determined automatically.

	Upper Jaw		Lower Jaw			
	Right	Left	Right	Left	Total	
					Right	Left
h-approach	0,61	0,56	0,56	0,62	0,59	0,59
					0,59	
v-approach	0,64	0,71	0,71	0,66	0,68	0,69
					0,69	

As stated above, the accuracy rates of the methods for both approaches are low when the main reference is determined automatically. The main reason for this is skipping the image enhancement step despite the inquality of the images. The reason of this omission is that it is not expected from the image enhancements methods to enhance the images effectively due to the strong noise effects in the images; but, at least, the image enhancement may correct the prediction inaccuracy of the main reference. We will study on this task in the future.

The results show that, the labelling method based on the bi-cost gives better results for both manual and automatic determination of the main reference, despite the fact that its accuracy is also not sufficient enough even the main reference.

There exist several reasons to obtain low accuracy rates: First, the sizes of the teeth in some of the test images are not well-balanced (Figure 6.10.a), especially on the upper jaw, that causes inconsistency between the tooth models and the images. Because, the graphical modelling approach used in our system considers that there is a certain increasing or decreasing rate between the teeth in an image. Second, the overlapped (Figure 6.10.b) and the uncoupled teeth (Figure 6.10.c) may be the reason of the incompatibility between the image and the model due to the same reason stated above.

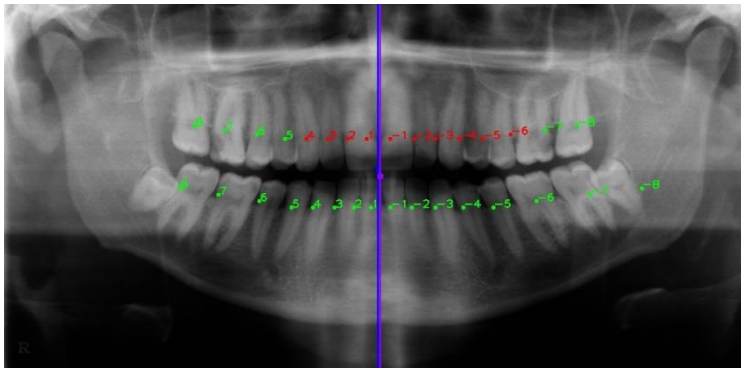

(a)

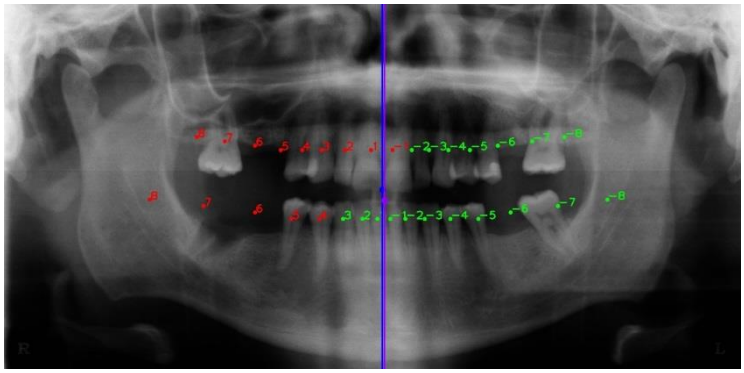

(b)

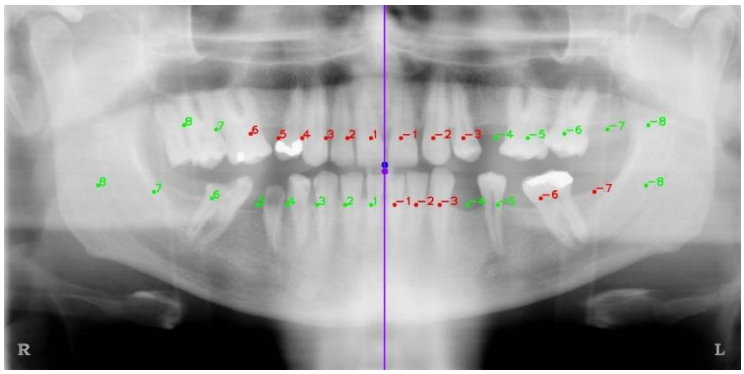

(c)

Figure 6.10 The visual results of three problematic images while labelling despite the main reference is determined manually, where the rate between the incisors and the molars is an exception in (a), the upper right premolars are overlapped in (b) and the position of the upper left canine is moved, and the teeth are uncoupled in (c).

On the other hand, the accuracy of the missing tooth determination is not acceptable due to skipping the image enhancement step. Therefore, the success of the missing tooth determination module was not computed. It is required to study on the enhancement of this process. However, it is expected to obtain better results for detection of the missing teeth after enhancing the images.

6.2.4 Benchmarking With a Well-Known Method

We applied the method of Wanat and Frejlichowski (Wanat and Frejlichowski, 2011a) to the same test images used in our system. In their method, they determine the gap position between adjacent teeth taking the neck position into account. The neck position is used against the overlapping problems on the crowns and the noise on the root locations. They, first, separate the upper and the lower jaw using the integral intensity projection horizontally in a particular region surrounding the center of the image. In order to find the horizontal center on the line determined as the mouth gap, the nose position is utilized. Then, instead of accepting the mouth gap as a horizontal line, they use spline function to find the separation curve between the jaws. The computation of the spline points is performed segment by segment in a particular width, initializing from the intersection of the mouth gap and the nose position. Afterwards, they move this spline vertically up to detect the dental pulps which are on nearly the same vertical position with the necks. Next, they apply a special filter to emphasize the gap position between the adjacent teeth. The integral intensity projection is used to determine the gaps aligned with the necks. Figure 6.11 shows the result of this method for the same test image presented above.

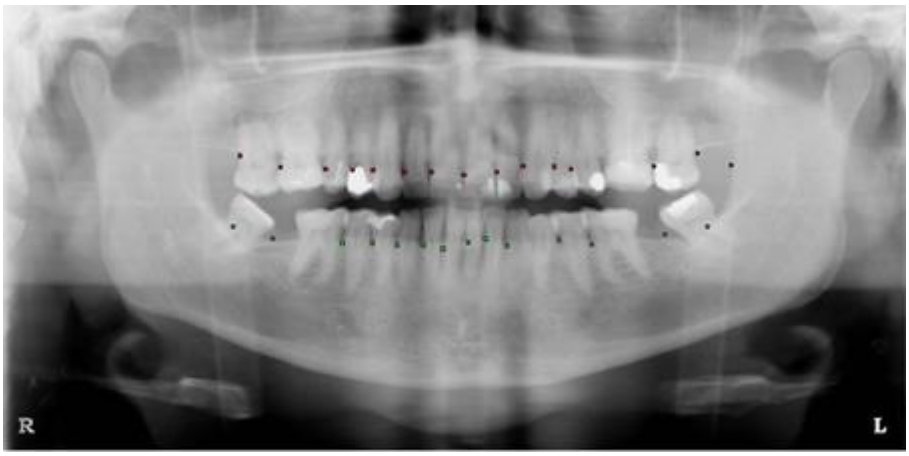

Figure 6.11 The visual result of the method of Wanat and Frejlichowski.

In their method, instead of labelling according to a numbering system, the gap positions are detected to segment the teeth individually (The method has following steps for this purpose which were not implemented due to the fact that these steps do not affect the labelling). However, we compare this method with ours based on the metric which computes the accuracy of the accurate predictions to all the teeth which is also used to compute the accuracy rate of our methods. When this method is used, in the right side of the upper jaw, 96 out of 139 teeth, in the left side of the upper jaw 81 out of 140 teeth, in the right side of the lower jaw, 118 out of 147 teeth, and in the left side of the lower jaw 104 out of 141 teeth are labelled accurately. Table 6.8 presents the results of the accuracy rates of this method.

Table 6.8. The numerical results of the method W & F (Wanat and Frejlichowski, 2011a).

Upper Jaw		Lower Jaw			
Right	Left	Right	Left	Total	
				Right	Left
0,69	0,58	0,80	0,74	0,64	0,77
				0,71	

It is seen that the acuracy rate of this method is better than our method when the main reference is determined automatically except the method based on the bi-cost with v-approach whose accuracy rate is same with this method. On the other hand, if the main reference is determined manullay in our system, despite of the fact that this method is again better than our method based on the d-cost for both the h-approach and the v-approach, it is worse than our method based on the bi-cost for both the h-approach and the v-approach. The differences between the accuracy rates of our methods and the method of Wanat and Frejlichowski (Wanat and Frejlichowski, 2011a) are a little when the main reference is determined manually (see Table 6.9).

Table 6.9 The benchmarking with our methods and the method of W & F (Wanat and Frejlichowski, 2011a).

			Upper Jaw		Lower Jaw			
			Right	Left	Right	Left	Total	
							Right	Left
manual main ref.	bi-cost	h-approach	0,73	0,69	0,75	0,77	0,71	0,76
							0,74	
		v-approach	0,72	0,69	0,86	0,78	0,70	0,82
							0,76	
	d-cost	h-approach	0,68	0,56	0,59	0,80	0,62	0,70
							0,66	
		v-approach	0,64	0,71	0,69	0,71	0,68	0,70
							0,69	
automatic main ref.	bi-cost	h-approach	0,55	0,56	0,61	0,52	0,56	0,57
							0,57	
		v-approach	0,74	0,71	0,67	0,69	0,73	0,68
							0,71	
	d-cost	h-approach	0,61	0,56	0,56	0,62	0,59	0,59
							0,59	
		v-approach	0,64	0,71	0,71	0,66	0,68	0,69
							0,69	
The method of W& F			0,69	0,58	0,80	0,73	0,64	0,77
							0,71	

The reasons of unsucces of this method on some images are similar with the ones for our method mentioned above; namely, the overlapped and uncoupled teeth, the un-balanced rate between the teeth, the missing teeth and the quality of the images. Figure 6.12 shows some images which are problematic for this method.

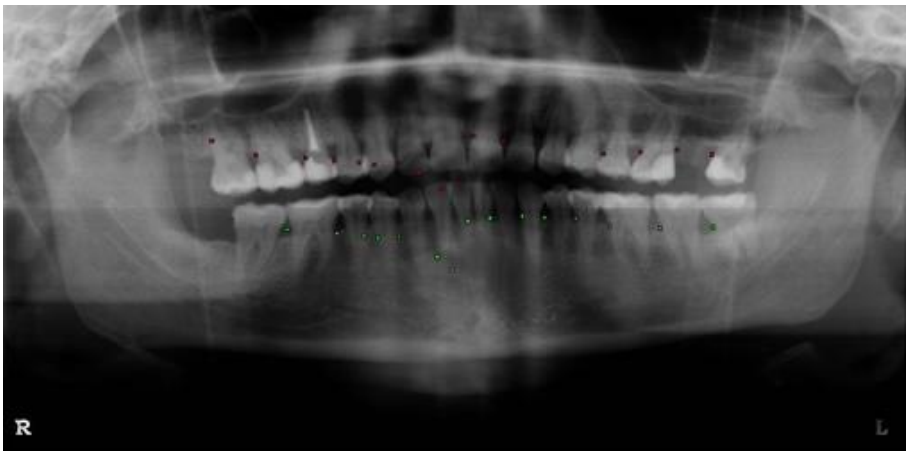

(a)

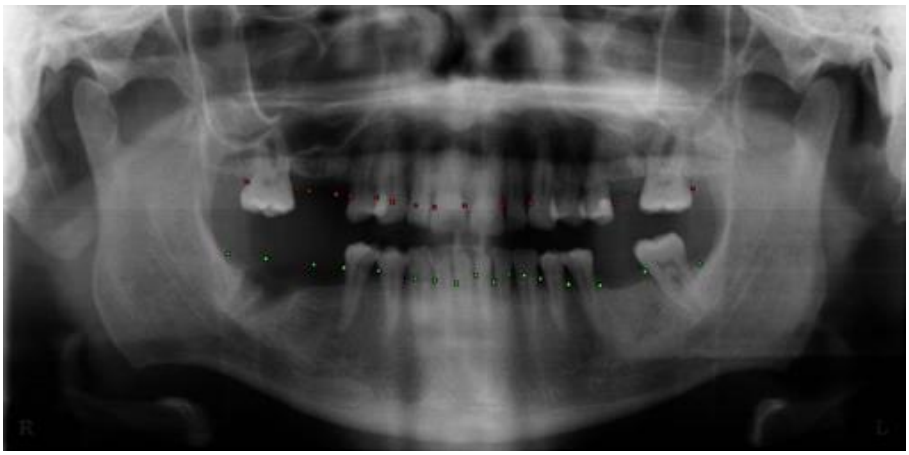

(b)

Figure 6.12 The visual results of the method of W & F for two problematic images where the gaps between the first incisor and the adjacent incisors in the right upper jaw are not detected which in (a), and the premolars are not separated due to overlapping in the left side of the upper jaw in (b).

6.2.5 The Discussion

We use the outputs of the detection module as input of the labelling module, therefore, the accuracy rate of the labelling module depends on the accuracy rate of the detection module. For that reason, in order to increase the accuracy rate of this module, it is required to produce better candidate tooth locations taking the considerations mentioned in the previous section into account. Alternatively, instead of trying to determine the tooth labels after the candidate detection, the feature extraction and classification may be employed based on the graphical tooth models constructed in this stage. Another approach is using a method such as the one of Wanat and Frejlichowski (Wanat and Frejlichowski, 2011a) presented above as the base method for this purpose. It means, the gap or the dental pulp locations may be used as the candidate tooth locations to be utilized for adapting an image to a tooth model.

As emphasized above, in order to construct a succesful fully automatic labelling module, it is required to enhance the image in a sufficient degree such that the main reference is detected accurately, and, as a result, the labelling is performed without any manual intervention.

Besides the improvements related to the image data and the main reference determination, the labelling methods themselves may be also improved by using different approaches. One suggestion is combining the methods used in the proposed system, namely, labelling considering both the bi-cost and the d-cost simultenously. It is expected to take sufficient results if the voting algorithms are utilized while combining the methods. Additionally, the construction logic of the tooth models may be improved by taking more specific characteristics of the teeth, such as the tooth angular position. Moreover, it is better to establish the model based on more than one reference. The number of the reference points might be increased using the most propable tooth locations as the additional references. Furthermore, the model construction may be implemented based on more complex graphical models such as the Markov Chain Model. Moreover, the number of the tooth models may be increased considering the changeable rate between the tooth widths. However, if it is aimed to get more impoved results, the labelling approach may be reformed, such that, instead of using a certain number of tooth models, 6 in our sytem, the tooth model is formulized and an optimizer

is established to produce a series of tooth models up to obtaining an acceptable cost (Figure 6.13). Namely, the labelling procedure may be thought as an optimization problem.

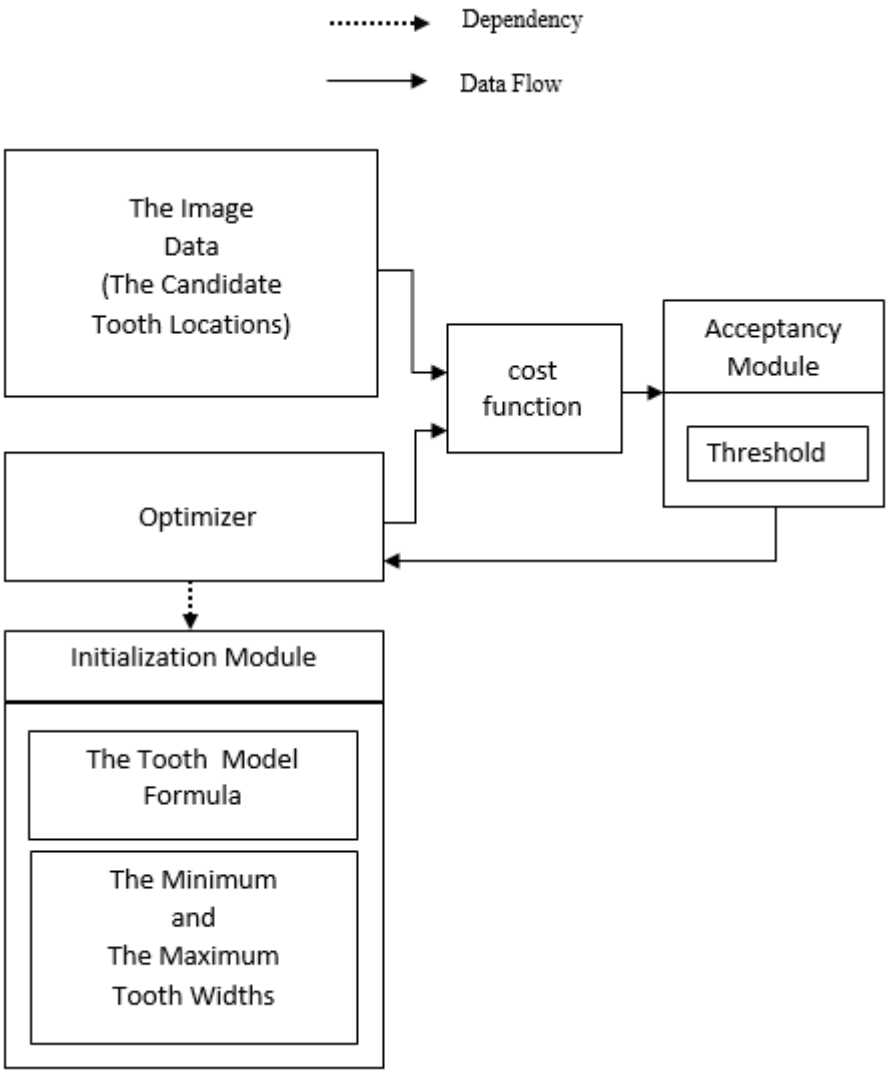

Figure 6.13 The Prospective Optimizer Based Labelling Approach.

CHAPTER 7

CONCLUSIONS

This study presents the tooth detection and the tooth labeling modules of a prospective human identification system. The system is designed for panoramic dental radiographs; however, it may be adapted to the other X-rays with small modifications.

The detection module extracts the Haar and the HOG feautures from the images, then, the SVM and the Boosting methods classify the teeth with the extracted features. After detection, the teeth are labelled by the pictorial structure like graphical models corresponding tooth numbering patterns. The labelling process is performed using dynamic programming with statistical optimization, the cost function minimization. Two cost functions were developed for tooth labelling both of which take the compatibility of the candidate tooth locations, detected by the detection module, with the corresponding tooth positons in the constructed graphical tooth models into account. They differ in relativity of computing the distances between the teeth; the first method mesures the distance between the adjacent teeth based on their own tooth centers, while the second method measures the distance according to the first incisor. For each method, within a series of tooth models, the most suitable tooth model is selected using two approaches; the model selection per tooth and the model selection for all the teeth in the processed image quadrant.

The proposed system was tested on 20 tooth images for both methods and both approaches mentioned above based on either manual or automatic determined main reference. When the main reference is determined manually, the accuracy rate for tooth location predictions for the first method is 74% while labelling the teeth based on a unique best model and 76% when the labelling is performed computing the best model

per tooth. The results of the second method is worse than the first one for each model selection approaches; 66% for the former approach and 64% for the later approach. On the other hand, when the main reference is determined automatically, the accuracy rates decrease as expected such that for the first method, the rate is 57% while the labelling is implemented based on a unique best model and 71% when the teeth are labelled by computing the best model per tooth. The results of the second method are 59% for the former approach and 69% for the later approach. The results show that automatic main reference determination needs to be improved to have a successful fully automatic system which we will study on as a future work.

We compare our results with the method of Wanat and Frejlichowski (Wanat and Frejlichowski, 2011a) which utilizes the dental pulp of the teeth for gap localization. The accuracy rates of our methods are close to this method whose accuracy rate is 71% on the same test images used in our system when the main reference is detected manually; however, this method is more successful than ours when the main reference in our system is detected automatically except the method finding the best tooth models per tooth using the cost function based on the processed tooth centers, whose accuracy rate is also 71%. The success of all methods is directly effected by the quality of the images, the overlapping and uncoupled teeth, the un-balanced rate between the teeth and the missing teeth in the test images.

We plan to study on raising the accuracy rate of the detection module by enhancing images using the suggested techniques in the literature, increasing the training data and handling the wisdom tooth as a separate tooth set. In addition, the tooth models in the labelling module will be also improved by taking numerous features such as the slopes of the teeth into account. Moreover, the labelling approaches will be enhanced such that the labelling is accepted as an optimization problem in which the tooth model corresponds the function whose characterists are tried to liken to the actual features of the teeth in the image. Furthermore, the determination of the missing tooth will be enhanced when the images are enhanced. The modules presented in this study will be the fundamental components of the prospective human identificaiton system which will be established to identify dead bodies after catastrophes comparing the antemortem and the postmortem images of the humans. It means, the results of this study will be utilized in the further stages of this sytem such as tooth matching.

REFERENCES

Abdel-mottaleb, M., Nomir,O, Nassar,D.E., Fahmy,G. and Ammar, H.H, "Challenges of Developing an Automated Dental Identification System", *IEEE 46th Midwest Symposium on Circuits and Systems*, Vol. 1, pp. 411-414, December 2003.

Bouzy, B., *Bagging and Boosting*, 2013, http://www.math-info.univ-paris5.fr/~bouzy/Doc/AA1/BaggingBoosting.pdf

Dalal, N. and Triggs, B., "Histograms of Oriented Gradients for Human Detection", *IEEE Computer Society Conference on Computer Vision and Pattern Recognition*, Vol. 1, pp. 886-893, June 2005.

Fahmy G., Nassar D., Haj-said E., Chen H., Nomir O., Zhou J., Howell R., Ammar H., Abdel-mottaleb M. and Jain A., "Towards An Automated Dental Identification System (ADIS)", *IEEE Biometrics Symposium*, Vol. 14, pp. 1-13, September 2006.

Freund, Y. and Schapire, R.E., *A Short Introduction to Boosting*, 1999, http://www.yorku.ca/gisweb/eats4400/boost.pdf

Frejlichowski, D. and Wanat, R., "Extraction of Teeth Shapes from Orthopantomograms for Forensic Human Identification", *Computer Analysis of Images and Patterns*, pp. 65-72, Springer Berlin Heidelberg, Berlin, 2011a.

Frejlichowski, D. and Wanat, R., "A Problem of Automatic Segmentation of Digital Dental Panoramic X-Ray Images for Forensic Human Identification", *Proceedings of CESCG 2011: The 15th Central European Seminar on Computer Graphics (CESCG)*, Vinič̆n, Slovakia, 2-4 May 2011, Vol. 1, pp. 165-172, Vienna University of Technology, Austria, 2011b.

Goa, H. and Chae, O., "Individual Tooth Segmentation from CT Images Using Level Set Method with Shape and Intensity Prior", *Pattern Recognition*, Vol. 43, pp. 2406-2417, July 2010.

Huang, P.W., Lin, P.L., Kuo, C. and Cho, Y.S., "An Effective Tooth Isolation Method for Bitewing Dental X-ray Images", *IEEE International Conference on Machine Learning and Cybernetics (ICMLC)*, Vol. 5, pp. 1814-1820, July 2012.

Huttenlocher, D.P. and Felzenszwalb P.F., "Pictorial Structures for Object Recognition", *International Journal of Computer Vision*, Vol. 61, pp. 55-79, January 2005.

Jain, A.K., Chen, H., "Matching of Dental X-ray Images for Human Identification", *Pattern Recognition*, Vol. 37, pp. 1519-1532, July 2004.

Jain A.K., Chen H., "Registration of Dental Atlas to Radiographs for Human Identification", *Proc. SPIE* 5779, *Biometric Technology for Human Identification II, 292*, Orlando, Florida, USA, 5 April 2005, Vol. 5779, pp. 292-298, SPIE, USA, 2005.

Kumar, B.S., "Boosting Techniques on Rarity Mining", *International Journal of Advanced Research in Computer Science and Software Engineering*, Vol. 2, pp. 27-35, October 2012.

Lin, P.L., Lai, Y.H. and Huang, P.W., "An Effective Classification and Numbering System for Dental Bitewing Radiograph Using The Region and Contour Information", *Pattern Recognition*, Vol. 43, pp. 1380-1392, April 2010.

Lira, P.H.M., Giraldi, G.A. and Neves, L.A.P., "Using the Mathematical Morphology and Shape Matching for Automatic Data Extraction in Dental X-Ray Images", *Anais-WVC 2013, VII Workshop de Visão Computacional*, Botafogo, Rio de Janeiro, Brazil, 3-5 June 2013, WVC, 2013.

Marana, A.N., Barboza, E.B. Papa, Hofer, M. and Oliveira, D.T., "Dental Biometrics for Human Identification, Biometrics", *Computer and Information Science, Human-Computer Interaction, Biometrcis-Unique and Diverse Applications in Nature, Science, and Technology*, Dr. Midori Albert (Ed.), ISBN: 978-953-307-187-9, InTech, DOI: 10.5772/15466, InTech, UK, 2013.

Mahoor M.H., Abdel-Mottaleb M., "Classification and Numbering of Teeth in Dental Bitewing Images", *Pattern Recognition*, Vol. 38, pp. 577-586, April 2005.

Petju, M., Suteerayongprasert, A., Thongpud, R. and Hassiri, K., "Importance of Dental Records for Victim Identification Following the Indian Ocean Tsunami Disaster in Thailand", *Public Health*, Vol. 121, pp. 251-257, April 2007.

Papageorgiou, C., Oren, M. and Poggio, T., "A General Framework for Object Detection", *Sixth International Conference on Computer Vision, 1998*, Bombay, Indian, 4-7 January 1998, pp. 555-562, IEEE, USA, 1998.

Pushparaj, V., Gurunathan, U. and Arumugam, B., "An Effective Dental Shape Extraction Algorithm Using Contour Information and Matching by Mahalanobis Distance", *Journal of Digital Imaging, Vol. 26, pp. 259, April* 2013.

Stanevski, N., Tsvetkov, D., "Using Support Vector Machine as a Binary Classifier", *International Conference on Computer Systems and Technologies - CompSysTech' 2005*, Varna, Bulgaria, 16-17 June 2005, DOI: 10.1.1.330.5058, CiteSeer, USA, 2005.

Schapire, R.H., "The Boosting Approach to Machine Learning: An Overview", *CiteSeer*, DOI: 10.1.1.24.5565, January 2002.

Seemann, E., *Histograms of Oriented Gradients*, 2008, http://www.docstoc.com/docs/159990563/Lecture-edgar-seemann-de

The Duy, N., Lamecker, H., Kainmueller, D. and Zachow, S., "Automatic Detection and Classification of Teeth in CT Data", *Medical Image Computing and Computer-Assisted Intervention – MICCAI 2012*, *15th International Conference*, Nice, France, 1-5 October 2012, Vol. 7510, pp. 609-616, Springer, US, 2012.

Viola, P., Jones, M., "Rapid Object Detection Using a Boosted Cascade of Simple Features", *Proceedings of the 2001 IEEE Computer Society Conference on Computer Vision and Pattern Recognition*, 2001, CVPR 2001, Vol. 1, pp. I-511 - I-518, DOI: 10.1109/CVPR.2001.990517, IEEE, USA, 2001.

Welling, M., *Support Vector Machines*, 2005, http://www.ics.uci.edu/~welling/classnotes/papers_class/SVM.pdf

Yuniarti, A., Nugroho, A.S., Amaliah, B. and Arifin, A.Z., "Classification and Numbering of Dental Radiographs for an Automated Human Identification System", *Telkomnika*, Vol. 10, No. 1, pp. 137-146, March 2012.